IMA Journal of Applied Mathematics (2023) **00**, 1–43
https://doi.org/10.1093/imamat/hxad005

Scattering resonances in unbounded transmission problems with sign-changing coefficient

Camille Carvalho
Department of Applied Mathematics, University of California, Merced, 5200 North Lake Road, Merced, CA 95343, USA
Univ Lyon, INSA Lyon, UJM, UCBL, ECL, CNRS UMR 5208, ICJ, F-69621, France

AND

Zoïs Moitier
POEMS, CNRS, Inria, ENSTA Paris, Institut Polytechnique de Paris, 828 Boulevard des Maréchaux, F-91120 Palaiseau, France
*Corresponding author: zois.moitier@ensta-paris.fr

[Received on 20 April 2022; revised on 06 December 2022; accepted on 2 January 2023]

It is well known that classical optical cavities can exhibit localized phenomena associated with scattering resonances, leading to numerical instabilities in approximating the solution. This result can be established via the 'quasimodes to resonances' argument from the black box scattering framework. Those localized phenomena concentrate at the inner boundary of the cavity and are called whispering gallery modes. In this paper we investigate scattering resonances for unbounded transmission problems with sign-changing coefficient (corresponding to optical cavities with negative optical properties, e.g. made of metamaterials). Due to the change of sign of optical properties, previous results cannot be applied directly, and interface phenomena at the metamaterial-dielectric interface (such as the so-called surface plasmons) emerge. We establish the existence of scattering resonances for arbitrary two-dimensional smooth metamaterial cavities. The proof relies on an asymptotic characterization of the resonances, and shows that problems with sign-changing coefficient naturally fit the black box scattering framework. Our asymptotic analysis reveals that, depending on the metamaterial's properties, scattering resonances situated close to the real axis are associated with surface plasmons. Examples for several metamaterial cavities are provided.

Keywords: Helmholtz Equation; Scattering resonances; Sign-changing coefficient; Asymptotic expansions;

2010 Math Subject Classification: 35P25; 35B40; 78A45.

1. Introduction

Unbounded transmission problems with sign-changing coefficients arise in electromagnetics, in particular when one considers Maxwell's equations in the time harmonic regime (with Transverse Electric or Transverse Magnetic polarization) in dielectric-metamaterial structures (typically a bounded metamaterial cavity surrounded by a dielectric). Contrary to common materials, metamaterials such as the Negative-Index Metamaterials (NIM) exhibit unusual optical properties: for instance a real-valued negative effective dielectric permittivity and/or a negative effective permeability at some frequency range. There is a great interest in modelling metamaterial cavities to confine and control light. In

particular, at optical frequencies, localized interface surface waves called surface plasmons can arise at dielectric-metamaterial interfaces (Maier, 2007). The field of plasmonics is very active as surface plasmons offer strong light enhancement, with applications to next-generation sensors, antennas, high-resolution imaging, cloaking and other (Sannomiya *et al.*, 2008). However, surface plasmons are very sensitive to the geometry and therefore challenging to capture, experimentally and numerically (Bonnet-Ben Dhia *et al.*, 2016; Helsing & Karlsson, 2018). Mathematically, surface plasmons are solutions of the homogeneous Maxwell's equations; they are oscillatory waves along the dielectric-metamaterial interface while exponentially decreasing in both transverse directions.

In classical transmission problems (meaning dielectric-dielectric structures), it has been shown that light can be confined by exciting the so-called whispering gallery modes (WGM) (Righini *et al.*, 2011). WGM are essentially supported in the neighborhood of the interior cavity boundary and are associated with *scattering resonances* (Balac *et al.*, 2021). It is well known that the approximation of light scattering in dielectric optical micro-cavities can be drastically affected by WGM, in particular if the excitation wavenumber of the source is close to a WGM resonance (Moiola & Spence, 2019; Balac *et al.*, 2021). In those cases the norm of the truncated solution operator explodes, which is observed numerically by the solution blowing-up (peaks): we call this *scattering instabilities*. Knowing the exact value of the scattering resonances is in general challenging (or impossible). However, one can obtain an asymptotic characterization of the scattering resonances, as done in Balac *et al.* (2021).

The above results do not directly apply to metamaterial cavities due to the change of sign of the optical parameter(s) and the additional interface plasmonic behaviours. There exists a framework that allows study of a large class of scattering problems, the so-called black box scattering framework. However, it is not immediately clear that unbounded transmission problems with sign-changing coefficients fit in this framework. In particular, well-posedness of the problem needs more attention, and spectral properties to define a *black box Hamiltonian* (including self-adjointness, lower semi-bound, etc.) may not be true. Also, surface plasmons have been mainly characterized and investigated in the context of the quasi-static approximation (*e.g.* Bonnet-Ben Dhia *et al.* (2013); Grieser (2014); Bonnet-Ben Dhia *et al.* (2016); Ammari *et al.* (2017); Carvalho *et al.* (2017); Bonnetier *et al.* (2019); Bonnet-Ben Dhia *et al.* (2021))—where an analytic expression can be found—therefore there is a need to obtain a characterization for the full problem (no quasi-static) to identify the associated metamaterial scattering resonances.

The goal of this paper is to establish the existence of metamaterial scattering resonances (causing scattering instabilities) via an asymptotic characterization of quasi-resonances (in other words the considered problems fit in the black box scattering framework), this for various two-dimensional metamaterial cavities (arbitrary smooth shape, with one arbitrary varying negative optical parameter). Using the T-coercivity theory (Bonnet-Ben Dhia *et al.*, 2012, 2013, 2016), and in the spirit of Balac *et al.* (2021), we establish that the associated spectral operator of scalar transmission problem with sign-changing coefficient is a black box Hamiltonian, and we carry out an asymptotic approximation of the metamaterial scattering resonances. In this case we find that there is an additional interface resonance family (compared with classical cavities) related to surface plasmons, and a specific scaling is required to asymptotically characterize them. This family can be located close to the real axis, and is responsible for scattering instabilities.

The paper is organized as follows. We present the problem and main results in Section 2. To illustrate the metamaterial scattering resonances and their effect, we provide a pedagogical example (case of a circular metamaterial cavity with constant negative coefficient) in Section 3. Section 4 presents the general approach for arbitrary metamaterial cavities, including the construction of the asymptotic approximation at any order. Section 5 proves their connection to the truncated solution

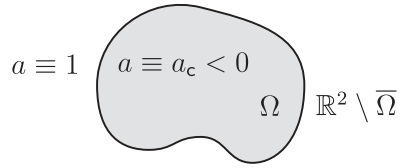

FIG. 1. Sketch of the geometry.

operator (extension of the 'quasimodes to resonances' result) and their consequence on scattering instabilities. Section 6 presents numerical illustrations of the metamaterial scattering resonances, and Section 7 presents our concluding remarks. Appendix A provides theoretical results about the problem operator, and Appendix B provides additional results and proofs needed in Section 4.

2. Problem setting and main result

2.1 *Mathematical settings*

Let us start by introducing the unbounded transmission problem with sign-changing coefficient, and its spectral analogous. We consider an open bounded connected set $\Omega \subset \mathbb{R}^2$ with a smooth boundary $\Gamma = \partial\Omega$ that represents a transparent (penetrable) optical *cavity* characterized by $a_c \in \mathscr{C}^\infty\big(\overline{\Omega}; (-\infty, 0)\big)$. The cavity is surrounded by a homogeneous background. We denote $a \in \mathrm{L}^\infty(\mathbb{R}^2)$ the piece-wise smooth function such that

$$a \equiv a_c \text{ on } \Omega \qquad \text{and} \qquad a \equiv 1 \text{ on } \mathbb{R}^2 \setminus \overline{\Omega}, \tag{2.1}$$

(see Fig. 1 for a sketch).

We consider the problem: For $f \in \mathrm{L}^2_{\mathrm{comp}}(\mathbb{R}^2)$, $g \in \mathrm{L}^2(\Gamma)$[1], and $k > 0$, find $u \in \mathrm{H}^1_{\mathrm{loc}}(\mathbb{R}^2)$ such that

$$\begin{cases} -\mathrm{div}\big(a^{-1}\,\nabla u\big) - k^2 u = f & \text{in } \mathbb{R}^2 \\ [u]_\Gamma = 0, \quad [a^{-1}\,\partial_n u]_\Gamma = g & \text{across } \Gamma \\ u \quad k\text{-outgoing} \end{cases} \tag{2.2}$$

and the associated spectral problem: Find $(\ell, u) \in \mathbb{C} \setminus \mathbb{R}_- \times \mathrm{H}^1_{\mathrm{loc}}(\mathbb{R}^2)$ such that $u \not\equiv 0$ and

$$\begin{cases} -\mathrm{div}\big(a^{-1}\,\nabla u\big) = \ell^2 u & \text{in } \mathbb{R}^2 \\ [u]_\Gamma = 0, \quad [a^{-1}\,\partial_n u]_\Gamma = 0 & \text{across } \Gamma \\ u \quad \ell\text{-outgoing} \end{cases}. \tag{2.3}$$

Above, $\mathrm{H}^1_{\mathrm{loc}}(\mathbb{R}^2) := \{u \in \mathrm{L}^2_{\mathrm{loc}}(\mathbb{R}^2) \,|\, \forall \chi \in \mathscr{C}^\infty_{\mathrm{comp}}(\mathbb{R}^2),\ \chi u \in \mathrm{H}^1(\mathbb{R}^2)\}$ and $n\colon \Gamma \to \mathbb{S}^1$ is the unit normal vector outward to Ω. Given X, we denote $[X]_\Gamma(\gamma) = \lim_{x \to \gamma^+} X(x) - \lim_{x \to \gamma^-} X(x)$, for any $\gamma \in \Gamma$, the jump condition across Γ. The jump conditions $[u]_\Gamma = 0$ and $[a^{-1}\,\partial_n u]_\Gamma = 0$ will be referred to as

[1] One could consider data in classical dual functional spaces. Then results presented here still hold.

the *transmission conditions*. We say that v is *k-outgoing* if it satisfies the outgoing wave condition:

$$v(r,\theta) = \sum_{m\in\mathbb{Z}} w_m(r)\,\mathrm{e}^{\mathrm{i}m\theta} = \sum_{m\in\mathbb{Z}} c_m \mathsf{H}_m^{(1)}(kr)\,\mathrm{e}^{\mathrm{i}m\theta} \tag{2.4}$$

with polar coordinates (r,θ) such that $r > \sup_{x\in\Omega}|x|$, $\theta \in \mathbb{R}/2\pi\mathbb{Z}$, $\mathsf{H}_m^{(1)}$ the Hankel function of the first kind of order m and $(c_m)_{m\in\mathbb{Z}} \in \mathbb{C}^{\mathbb{Z}}$. For a pair (ℓ, u) solution of Equation (2.3), ℓ is called a *scattering resonance* and the function u is a *resonant mode* associated with ℓ.

We define $P\colon u \mapsto -\mathrm{div}(a^{-1}\nabla u)$ the $\mathrm{L}^2(\mathbb{R}^2)$ operator from Equation (2.3) with the domain $\mathcal{D}(P) := \{u \in \mathrm{L}^2(\mathbb{R}^2) \,|\, \mathrm{div}(a^{-1}\nabla u) \in \mathrm{L}^2(\mathbb{R}^2)\}$[2]. We also define the local version of the domain $\mathcal{D}_{\mathrm{loc}}(P) := \{u \in \mathrm{L}^2_{\mathrm{loc}}(\mathbb{R}^2) \,|\, \forall \chi \in \mathscr{C}^\infty_{\mathrm{comp}}(\mathbb{R}^2),\ \chi u \in \mathcal{D}(P)\}$.

For classical cavities ($a_{\mathsf{c}} > 0$), one can show that Equation (2.2) is well-posed in $\mathrm{H}^1_{\mathrm{loc}}(\mathbb{R}^2)$, the operator $(P, \mathcal{D}(P))$ is self-adjoint, its spectrum is real and admits a lower bound. This allows us in particular to work in the framework of the *black box scattering* (Dyatlov & Zworski, 2019, Definition 4.6), where one can check that there is an underlying *black box Hamiltonian* (see Lemma 5.2 for more details). We can define $\mathfrak{Res}\colon k \mapsto \left(P - k^2\right)^{-1}$ the resolvent[3] associated with P. An asymptotic characterization of the scattering resonances close to the real axis (called *quasi-resonances* $\underline{k}_m$) is provided in Balac *et al.* (2021), and with the 'quasimodes to resonances' result (Stefanov & Vodev, 1995, 1996; Tang & Zworski, 1998; Stefanov, 1999), it is proved that true resonances $(\ell_m)_m$ are super-algebraically close to quasi-resonances $\underline{k}_m$. As a consequence the solution of Equation (2.2) blows up for $k = \underline{k}_m$ (and the norm of the truncated resolvent $\mathfrak{Res}(\underline{k}_m)$ explodes).

Due to the change of sign of a, the 'quasimodes to resonances' result from the black box scattering framework does not directly apply in our case. First, well-posedness of Equation (2.2) in $\mathrm{H}^1_{\mathrm{loc}}(\mathbb{R}^2)$ is not guaranteed as $u \mapsto -\mathrm{div}(a^{-1}\nabla u)$ does not necessarily define a Fredholm operator (or in other words the coercivity of the associated weak form of Equation (2.2) is not guaranteed). Additionally, spectral requirements on P to be a black box Hamiltonian are not obvious. Finally, it is not clear whether there exist resonances close to the real axis that are associated with localized interface modes (potentially related to surface plasmons).

The goal of this paper is to show that the 'quasimodes to resonances' result still applies for unbounded transmission problems with sign-changing coefficient, and to provide an asymptotic characterization of the scattering resonances.

Remark 2.1.

- The k-outgoing condition defined in Equation (2.4) is equivalent to v satisfying the so-called Sommerfeld radiation condition if and only if $k > 0$. This outgoing condition is more general, and will be also used for the associated spectral problem Equation (2.3), where one can have ℓ-outgoing solutions with $\ell \in \mathbb{C} \setminus \mathbb{R}_-$.
- The fact that we look for $\ell \in \mathbb{C} \setminus \mathbb{R}_-$ allows us to work on the logarithmic plane. This guarantees analyticity of the Hankel function (Olver *et al.*, 2010, Chapter 10), and it is necessary for spectral

[2] One can show that $\mathcal{D}(P) = \{u \in \mathrm{H}^1(\mathbb{R}^2) \,|\, \Delta\, u|_\Omega \in \mathrm{L}^2(\Omega),\ \Delta\, u|_{\mathbb{R}^2\setminus\overline{\Omega}} \in \mathrm{L}^2(\mathbb{R}^2 \setminus \overline{\Omega}),\ [a^{-1}\partial_n u]_\Gamma = 0\}$ (see Lemma A.1). This second definition will be heavily used in Section 5.

[3] $\mathfrak{Res}$ is defined on the upper half of the complex plane ($\Im(k) > 0$). Using the *black box scattering* framework (see Dyatlov & Zworski (2019)), we can extend the resolvent to $\mathbb{C} \setminus \mathbb{R}_-$.

problems set in spaces of even dimension (Dyatlov & Zworski, 2019, Definition 4.6), typically Equation (2.3) set in $\mathbb{R}^2$.

- Depending on the polarization (TE / TM), the optical cavity is characterized by a permittivity $a = \varepsilon$ and a permeability $\mu = 1$ or a permeability $a = \mu$ and a permittivity $\varepsilon = 1$. Metamaterials are commonly characterized by $\varepsilon < 0$ and/or $\mu < 0$. The cavity is embedded in a normalized homogeneous background characterized by $\mu = 1$, and $\varepsilon = 1$.
- Equation (2.2) includes the scattering by a plane wave.

2.2 *Main result*

Our main goal is to establish the existence of a discrete sequence of scattering resonances close to the positive real axis, which is done in two steps. First, we derive approximate solutions of the resonance problem Equation (2.3) called *quasi-pairs* (Balac *et al.*, 2021, Definition 2.1) (Theorem 2.3); then we show that there exist true resonances close to the approximate ones (Theorem 2.4), which rely on showing that the 'quasimodes to resonances' result from the black box scattering applies for Equation (2.3). For ease of reading, we (re)define quasi-pairs as follows:

DEFINITION 2.2. A *quasi-pair* for the resonance problem Equation (2.3) is formed by a sequence $(\underline{\lambda}_m)_{m\geq 1}$ of real numbers, and a sequence $(\underline{u}_m)_{m\geq 1}$ of complex valued functions that satisfy the following conditions:

1. For any $m \geq 1$, the functions $\underline{u}_m$ are uniformly compactly supported and
$$\underline{u}_m \in \mathcal{D}(P), \quad \text{with} \quad \|\underline{u}_m\|_{\mathrm{L}^2(\mathbb{R}^2)} = 1.$$
2. We have the following quasi-pair estimate
$$\|P\underline{u}_m - \underline{\lambda}_m \underline{u}_m\|_{\mathrm{L}^2(\mathbb{R}^2)} = \mathcal{O}\big(m^{-\infty}\big), \qquad \text{as } m \to +\infty, \tag{2.5}$$
with the notation $a_m = \mathcal{O}(m^{-\infty})$ to indicate that for all $N \in \mathbb{N}$, there exists $C_N > 0$ such that $|a_m| \leq C_N\, m^{-N}$, for all $m \geq 1$.
3. Additionally, we say that $\underline{u}_m$ is localized around $\Gamma \subset \mathbb{R}^2$ if, for all $\delta > 0$, its support is mainly in $\Gamma_\delta := \{x \in \mathbb{R}^2 \,|\, \mathrm{dist}(x, \Gamma) < \delta\}$ neighborhood of Γ in the sense that
$$\|\underline{u}_m\|_{\mathrm{L}^2(\Gamma_\delta)} = 1 - \mathcal{O}\big(m^{-\infty}\big), \qquad \text{as } m \to +\infty. \tag{2.6}$$

We call $\big(\underline{u}_m\big)_{m\geq 1}$ quasi-modes, and $\big(\underline{k}_m := \sqrt{\underline{\lambda}_m}\big)_{m\geq 1}$ quasi-resonances.

THEOREM 2.3. If $a_{\mathsf{c}}(\gamma) \neq -1$, for all $\gamma \in \Gamma$, then we can construct $\big(\underline{\lambda}_m, \underline{u}_m\big)_{m\geq 1}$ quasi-pairs of the resonance problem Equation (2.3). Moreover, we have $\underline{\lambda}_m = \left(\frac{2\pi m}{L}\right)^2 \Lambda\big(\frac{L}{2\pi m}\big)$, where L is the length of the curve Γ and $\Lambda \in \mathscr{C}^\infty\big(\big[0, \frac{L}{2\pi}\big]\big)$ (see Equation (4.16a)). The quasi-mode is of the form $\underline{u}_m = \exp\left(\mathrm{i}\frac{2\pi m}{L}\,\Theta\right)\Phi$ with Θ, Φ smooth functions with respect to $\frac{L}{2\pi m}$ and Φ is exponentially decreasing on

both sides of the interface Γ (see Equation (4.16b)). Additionally, the sign of $\underline{\lambda}_m$ is given to leading order by the sign of $1 + a_{\mathsf{c}}|_{\Gamma}^{-1}$, and $\big(\underline{\lambda}_m\big)_{m\geq 1}$ are independent of the construction.

THEOREM 2.4. If $a_{\mathsf{c}}(\gamma) \neq -1$, for all $\gamma \in \Gamma$, let $\big(\underline{\lambda}_m, \underline{u}_m\big)_{m\geq 1}$ be the quasi-pairs of Theorem 2.3. Then there exists a sequence of true scattering resonances $\big(\ell_m\big)_{m\geq 1}$ of Equation (2.3) close to the quasi-resonances $\big(\sqrt{\underline{\lambda}_m}\big)_{m\geq 1}$ in the sense that

$$\ell_m^2 = \underline{\lambda}_m + \mathcal{O}\big(m^{-\infty}\big), \qquad \text{as } m \to +\infty.$$

In addition:

- If $a_{\mathsf{c}}(\gamma) < -1$, for all $\gamma \in \Gamma$, then $\big(\ell_m\big)_{m\geq 1}$ are scattering resonances with $\Re\big(\ell_m\big) > 0$ and $-1 \ll \Im\big(\ell_m\big) < 0$.
- If $-1 < a_{\mathsf{c}}(\gamma) < 0$, for all $\gamma \in \Gamma$, then $\ell_m \in \mathrm{i}\mathbb{R}_+$, $\forall m \geq 1$, and $\big(\ell_m^2\big)_{m\geq 1}$ are negative eigenvalues.

From Definition 2.2, recall that $a_m = \mathcal{O}(m^{-\infty})$ indicates that for all $N \in \mathbb{N}$, there exists $C_N > 0$ such that $|a_m| \leq C_N\, m^{-N}$, for all $m \geq 1$. Then Theorems 2.3 and 2.4 provide asymptotic estimates, which imply:

- $\big(\underline{\lambda}_m\big)_{m\geq 1}$ are independent of the construction in the sense that, if one has two quasi-resonances $(\underline{\lambda}_m)_{m\geq 1}, (\underline{\mu}_m)_{m\geq 1}$ corresponding to the same integer m, then $\underline{\lambda}_m - \underline{\mu}_m = \mathcal{O}(m^{-\infty})$. This is demonstrated in Corollary 4.13.
- Estimates $\ell_m^2 = \underline{\lambda}_m + \mathcal{O}\big(m^{-\infty}\big)$ naturally provide less accurate result for small m. Some numerical illustrations will be provided in Section 6.

Contrary to the classical cavities ($a_{\mathsf{c}} > 0$), the value of a_{c} can lead to two different behaviours: from Theorems 2.3 and 2.4 we only have one sequence of resonances $\big(\ell_m\big)_{m\geq 1}$ close to the positive real axis (in the ℓ_m plane) in the case $a_{\mathsf{c}}(\gamma) < -1$ (where we built $(\underline{k}_m)_m \in \mathbb{R}^+$), and none in the case $-1 < a_{\mathsf{c}}(\gamma) < 0$ (where we obtained $(\underline{k}_m)_m \in \mathrm{i}\mathbb{R}$), see Moitier (2019); Balac *et al.* (2021). From Theorem 2.4 one can show that the truncated resolvent explodes at the quasi-resonances, and thus scattering instabilities occur for Equation (2.2).

COROLLARY 2.5. If $a_{\mathsf{c}}(\gamma) < -1$, for all $\gamma \in \Gamma$, then there exists a real sequence $\big(\underline{k}_m\big)_{m\geq 1}$ with $\lim_{m\to+\infty} \underline{k}_m = +\infty$ such that for all $\chi \in \mathscr{C}^\infty_{\mathrm{comp}}(\mathbb{R}^2)$ with $\chi \equiv 1$ on an open neighborhood of $\overline{\Omega}$ and for all $N \in \mathbb{N}$, there exists a constant $C_N > 0$,

$$\big|\!\big|\!\big| \chi\, \mathfrak{Res}(\underline{k}_m)\, \chi \big|\!\big|\!\big| \geq C_N m^N, \qquad \forall m \geq 1.$$

The above results also rely on well-posedness of Equation (2.2), and on establishing that P is a black box Hamiltonian. This can be done using the T-coercivity framework (Bonnet-Ben Dhia *et al.*, 2012, 2013, 2016), allowing to compensate for the change of sign of a and establishing Fredholm properties (and others) under some conditions. Section 5 and Appendix A detail those results. Well-posedness of Equation (2.2) in Hadamard's sense leads to the existence of a stability constant $C(k) > 0$ such that $\|u\|_{\mathrm{L}^2(\mathbb{D}(0,\rho))} \leq C(k)(\|f\|_{\mathrm{L}^2(\mathbb{R}^2)} + \|g\|_{\mathrm{L}^2(\Gamma)})$, for any open disk such that $\overline{\Omega} \cup \mathrm{supp}(f) \subset \mathbb{D}(0,\rho)$, see Lemma A.4. From Corollary 2.5 we deduce the following:

COROLLARY 2.6. If $a_{\mathsf{c}}(\gamma) < -1$, for all $\gamma \in \Gamma$, then there exists a real sequence $\left(\underline{k}_m\right)_{m\geq 1}$ with $\lim_{m\to+\infty} \underline{k}_m = +\infty$ such that for all $N \in \mathbb{N}$, there exists a constant $C_N > 0$,

$$C\left(\underline{k}_m\right) \geq C_N m^N, \qquad \forall m \geq 1.$$

Equation (2.2) suffers from scattering instabilities for $k = \underline{k}_m$.

The construction of the real sequence $\left(\underline{\lambda}_m\right)_m$ (consequently $\left(\underline{k}_m\right)_m$) is the fundamental element in the above results. To illustrate how to proceed, we present a simple case in Section 3 where all calculations can be done explicitly, and we generalize the approach to arbitrary smooth cavities in Section 4.

3. A pedagogical example

In this section we consider Equation (2.2) set on a circular cavity with constant negative a_{c}: Ω is a disk of radius $R > 0$, and $a_{\mathsf{c}} = -\eta^2$ with $\eta > 0$. Taking advantage of the geometry, we look for solution of the form:

$$u(x) = u(r,\theta) = \sum_{m\in\mathbb{Z}} u_m(r,\theta) = \sum_{m\in\mathbb{Z}} w_m(r)\, \mathsf{e}^{\mathsf{i}m\theta}, \tag{3.1}$$

with $(r,\theta) \in \mathbb{R}_+ \times \mathbb{R}/2\pi\mathbb{Z}$ the polar coordinates corresponding to the Cartesian coordinates x, and $w_m(r) = \frac{1}{2\pi}\int_0^{2\pi} u(r,\theta)\, \mathsf{e}^{-\mathsf{i}m\theta}\mathrm{d}\theta$, $m \in \mathbb{Z}$, the angular Fourier coefficients. Similarly, we assume we can write $f(x) = \sum_{m\in\mathbb{Z}} f_m(r)\, \mathsf{e}^{\mathsf{i}m\theta}$, for $x \in \mathbb{R}^2$ with $f_m \in \mathrm{L}^2_{\mathrm{comp}}(\mathbb{R})$, and we can write $g(x) = \sum_{m\in\mathbb{Z}} g_m\, \mathsf{e}^{\mathsf{i}m\theta}$, for $x \in \Gamma$ with $g \in \mathrm{L}^2(\Gamma)$.

REMARK 3.1. An example where Equation (2.2) naturally arises is the scattering by a transparent obstacle of a plane wave. If one considers $u^{\mathsf{in}}(x_1,x_2) = \mathsf{e}^{\mathsf{i}kx_2}$, with wavenumber k and direction $(0,1)^\intercal$, then Equation (2.2) is satisfied by the scattered field $u^{\mathsf{sc}} := u - u^{\mathsf{in}}$ with data $f^{\mathsf{in}} := \mathrm{div}\left(a^{-1}\nabla u^{\mathsf{in}}\right) + k^2 u^{\mathsf{in}}$ and $g^{\mathsf{in}} := -[a^{-1}\,\partial_n u^{\mathsf{in}}]_\Gamma$. Additionally, one can check that f_m is supported only in the cavity: $f_m(r) = k^2(1 - a_{\mathsf{c}}^{-1})\mathsf{J}_m(k\,r)$, $r \in (0,R)$, where J_m denotes the Bessel function of the first kind of order m. This expansion is obtained using the Jacobi–Anger expansion of u^{in} (Olver *et al.*, 2010, Eq. 10.12.1) that converges absolutely on every compact set of $\mathbb{R}^2$.

Plugging Equation (3.1) in Equation (2.2), we obtain a family of 1D problems indexed by $m \in \mathbb{Z}$: Find $w_m \in \mathrm{H}^1_{\mathrm{loc}}(\mathbb{R}_+, r\mathrm{d}r)$ such that

$$\begin{cases} -\frac{1}{r}\partial_r\left(r\,\partial_r w_m\right) + \dfrac{m^2}{r^2} w_m - a_{\mathsf{c}} k^2\, w_m = a_{\mathsf{c}} f_m & \text{in } (0,R) \\ -\frac{1}{r}\partial_r\left(r\,\partial_r w_m\right) + \dfrac{m^2}{r^2} w_m - k^2\, w_m = f_m & \text{in } (R,+\infty) \\ [w_m]_\Gamma = 0, \quad [a^{-1}\, w_m']_{\{R\}} = g_m & \text{across } \{R\} \\ w_0'(0) = 0 \quad \text{or} \quad w_m(0) = 0 \text{ for } m \neq 0 & \text{on } \{0\} \\ w_m(r) \propto \mathsf{H}^{(1)}_m(kr) & r > R \end{cases} \tag{3.2}$$

with $\propto$ meaning 'up to a constant'. For $m \neq 0$, the term $\frac{m^2}{r^2} w_m$ imposes a homogeneous Dirichlet boundary condition at zero (Bernardi *et al.*, 1999). The solution is continuous at $r = 0$, using the

outgoing wave condition we write

$$w_m(r) = \begin{cases} \alpha_m \frac{\mathsf{I}_m(\eta\, k\, r)}{\mathsf{I}_m(\eta\, k\, R)} + f_{a_\mathsf{c}}(r), & \text{if } r \le R, \\ \beta_m \frac{\mathsf{H}^{(1)}_m(k\, r)}{\mathsf{H}^{(1)}_m(k\, R)} + f_R(r), & \text{if } r > R, \end{cases} \tag{3.3}$$

with I_m denoting the modified Bessel function of the first kind of order m, and f_{a_c}, f_R denoting particular solutions. Our goal in this section is to investigate the associated operator (in particular the resolvent operator), therefore we do not need to write the particular solutions explicitly. Above, the coefficients (α_m, β_m) are the solution of

$$A^\eta_m(kR)\begin{pmatrix}\alpha_m \\ \beta_m\end{pmatrix} = \begin{pmatrix} f_{a_\mathsf{c}}(R) - f_R(R) \\ g_m + a_\mathsf{c}^{-1} f'_{a_\mathsf{c}}(R) - f'_R(R)\end{pmatrix}, \; A^\eta_m(z) = \begin{pmatrix} 1 & -1 \\ -\frac{1}{\eta}\frac{\mathsf{I}'_m(\eta\, z)}{\mathsf{I}_m(\eta\, z)} & -\frac{\mathsf{H}^{(1)\prime}_m(z)}{\mathsf{H}^{(1)}_m(z)}\end{pmatrix}. \tag{3.4}$$

The above system comes from the transmission conditions at $r = R$.

Remark 3.2. Since $k > 0$ and the problem is well-posed for $\eta \neq 1$ (see Lemma A.4), coefficients (α_m, β_m) are uniquely defined and $\det(A^\eta_m(kR)) \neq 0$, with

$$\det(A^\eta_m(z)) := -\eta^{-1}\frac{\mathsf{I}'_m(\eta\, z)}{\mathsf{I}_m(\eta\, z)} - \frac{\mathsf{H}^{(1)\prime}_m(z)}{\mathsf{H}^{(1)}_m(z)}, \quad \forall z \in \mathbb{C}^*. \tag{3.5}$$

Now that we have an explicit expression of $\big(A^\eta_m(kR)\big)_{m\in\mathbb{Z}}$, we can analyse its behaviour for various wavenumbers k and values of a_c (namely η). For numerical purposes, we truncate Equation (3.1) to order M, leading to consider the sequence of operators $\big(A^\eta_{-M}(kR), \ldots, A^\eta_0(kR), \ldots, A^\eta_M(kR)\big)$. We choose here $M = 32$ and $R = 1$. The resolvent of this spectral numerical scheme is $\mathbb{A}_k^{-1}$, where

$$\mathbb{A}_k := \operatorname{diag}\big(A^\eta_{-M}(kR), \ldots, A^\eta_0(kR), \ldots, A^\eta_M(kR)\big). \tag{3.6}$$

To look at the stability of this scheme, we look at the spectral norm of $\mathbb{A}_k^{-1}$ noted $\left|\!\left|\!\left|\mathbb{A}_k^{-1}\right|\!\right|\!\right|_2$. Figure 2 represents the log plot of $\left|\!\left|\!\left|\mathbb{A}_k^{-1}\right|\!\right|\!\right|_2$ with respect to k, for various values of a_c. One observes that there exists a sequence $(k_m)_m$ such that $\left|\!\left|\!\left|\mathbb{A}_{k_m}^{-1}\right|\!\right|\!\right|_2$ peaks when $a_\mathsf{c} \in (-\infty, -1)$, while $\left|\!\left|\!\left|\mathbb{A}_k^{-1}\right|\!\right|\!\right|_2$ remains bounded when $a_\mathsf{c} \in (-1, 0)$. In the first case, the sequence $\left(\left|\!\left|\!\left|\mathbb{A}_{k_m}^{-1}\right|\!\right|\!\right|_2\right)_{m\ge1}$ grows exponentially (Moiola & Spence, 2019; Hiptmair *et al.*, 2022). We refer to those peaks as *scattering instabilities*.

The above results provide the following:

- While Equation (2.2) is well-posed for all $k > 0$, the associated resolvent operator explodes for a sequence of wavenumbers $\big(k_m\big)_{m\ge1}$.
- This phenomenon occurs only for $a_\mathsf{c} < -1$.

In what follows, we investigate the associated spectral problem to identify the resonances causing the scattering instabilities. We then use semi-classical analysis to characterize the sequence $\big(k_m\big)_{m\ge1}$, and study their relationship to surface plasmons.

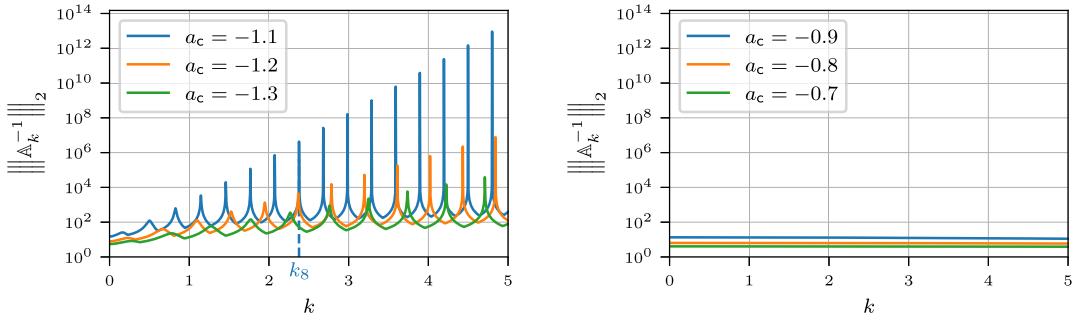

$a_c \in \{-1.3, -1.2, -1.1\}$ $a_c \in \{-0.9, -0.8, -0.7\}$

FIG. 2. Semi-log plot of the function $k \mapsto \left\|\mathbb{A}_k^{-1}\right\|_2$ with respect to $k > 0$ for $a_c \in \{-1.3, -1.2, -1.1\}$ (left), for $a_c \in \{-0.9, -0.8, -0.7\}$ (right). The value k_8 marked on the graph corresponds to the reference value used in Fig. 4 and 6.

3.1 *Scattering resonances for the disk*

As done in the previous section, Equation (2.3) set on a disk can be rewritten as a family of one-dimensional problems indexed by $m \in \mathbb{Z}$: Find $(\ell, w_m) \in \mathbb{C} \setminus \mathbb{R}_- \times \mathrm{H}^1_{\mathrm{loc}}(\mathbb{R}_+, r\mathrm{d}r) \setminus \{0\}$, such that

$$\begin{cases} -\frac{1}{r}\partial_r\big(r\,\partial_r w_m\big) + \dfrac{m^2}{r^2} w_m - a_c \ell^2\, w_m = 0 & \text{in } (0,R) \\ -\frac{1}{r}\partial_r\big(r\,\partial_r w_m\big) + \dfrac{m^2}{r^2} w_m - \ell^2\, w_m = 0 & \text{in } (R,+\infty) \\ [w_m]_\Gamma = 0, \quad [a^{-1} w_m']_{\{R\}} = 0 & \text{across } \{R\} \\ w_0'(0) = 0 \quad \text{or} \quad w_m(0) = 0 \text{ for } m \neq 0 & \text{on } \{0\} \\ w_m(r) \propto \mathsf{H}_m^{(1)}(\ell r) & r > R \end{cases} \tag{3.7}$$

Similarly, we write

$$w_m(r) = \begin{cases} \alpha_m \dfrac{\mathsf{I}_m(\eta\,\ell\,r)}{\mathsf{I}_m(\eta\,\ell\,R)}, & \text{if } r \leq R, \\ \beta_m \dfrac{\mathsf{H}_m^{(1)}(\ell\,r)}{\mathsf{H}_m^{(1)}(\ell\,R)}, & \text{if } r > R, \end{cases} \tag{3.8}$$

however this time, the pair (ℓ, w_m) is solution of Equation (3.7) if and only if there exists $(\alpha_m, \beta_m)^\intercal \in \ker\left(A_m^\eta(\ell R)\right) \setminus (0,0)^\intercal$, with $A_m^\eta(\ell R)$ defined in Equation (3.4). Given $m \in \mathbb{Z}$, and using Equation (3.5), we define the set of resonances

$$\mathcal{R}[a_c, R](m) = \{\ell \in \mathbb{C} \setminus \mathbb{R}_- \mid \det\left(A_m^\eta(\ell R)\right) = 0\}. \tag{3.9}$$

Finally, we define the set of resonances of Equation (2.3)

$$\mathcal{R}[a_c, R] := \bigcup_{m \in \mathbb{Z}} \mathcal{R}[a_c, R](m). \tag{3.10}$$

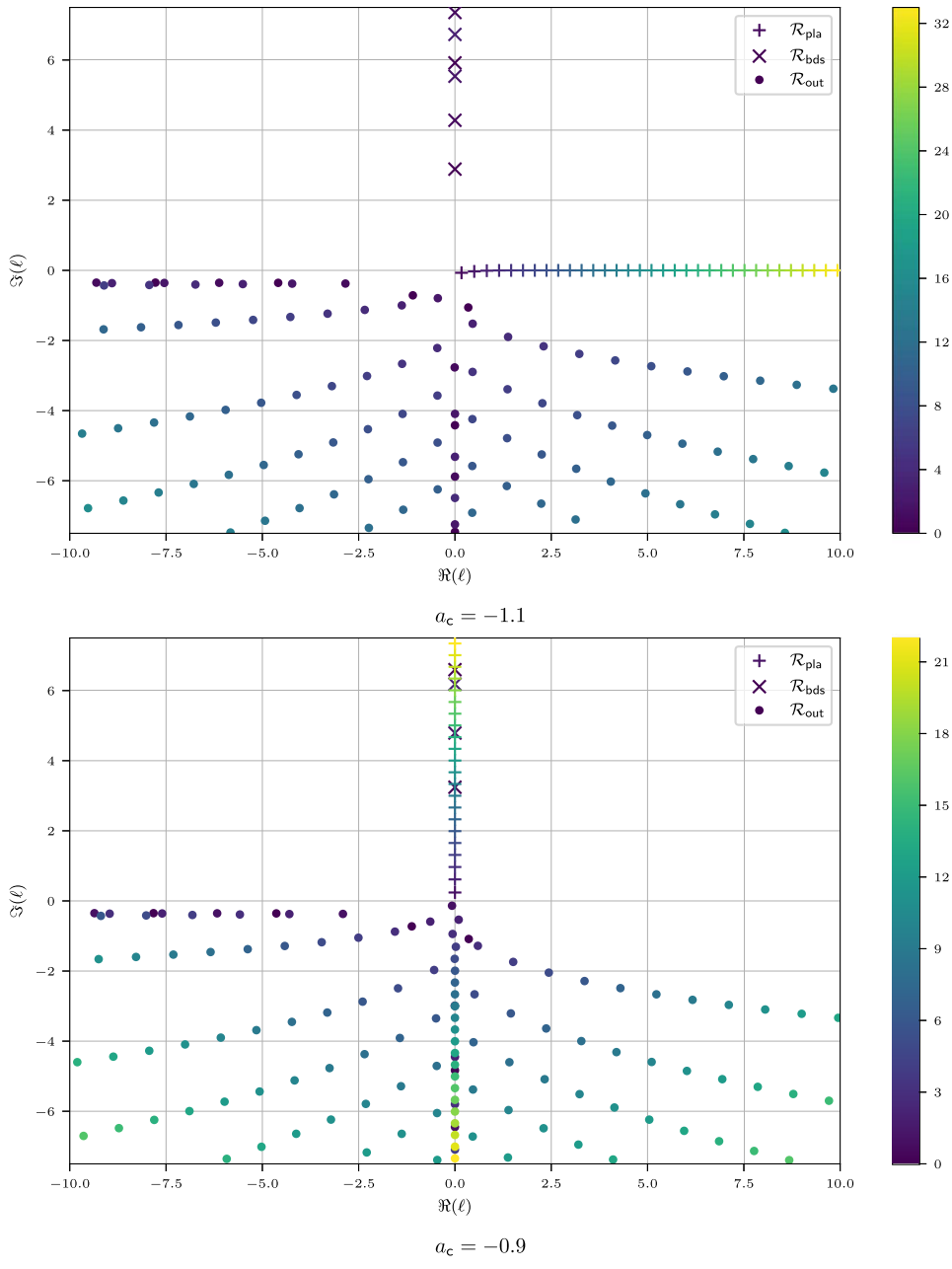

FIG. 3. Graph of the sets $\mathcal{R}_{33}[-1.1, 1]$ (top) and $\mathcal{R}_{22}[-0.9, 1]$ (bottom) in the complex plane $(\Re(\ell), \Im(\ell))$ with $\ell \in \mathbb{C} \setminus \mathbb{R}_-$. Those sets are computed using complex contour integration Parini (2018) on the analytic function in Equation (3.5).

REMARK 3.3. Given $\ell \in \mathcal{R}[a_c, R](m)$, one finds $\alpha_m = c$ and $\beta_m = c$ with $c \in \mathbb{C}^*$ since the resonant modes are defined up to some normalization.

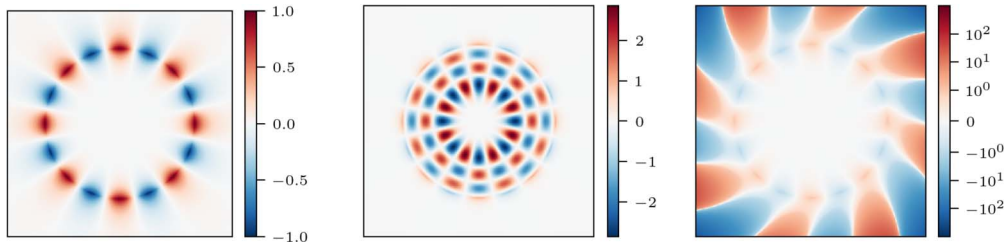

FIG. 4. Real part of some resonant modes $u_8(r,\theta)$ for $a_{\mathsf{c}} = -1.1$ with their corresponding resonances below.

REMARK 3.4. Since $\mathsf{I}_{-m} = \mathsf{I}_m$ and $\mathsf{H}^{(1)}_{-m} = (-1)^m \mathsf{H}^{(1)}_m$, for all $m \in \mathbb{Z}$, see (Olver *et al.*, 2010, Eq. 10.27.1 and 10.4.2), by symmetry all the resonances ℓ, corresponding to $m \neq 0$, are of multiplicity 2, and the two associated modes are conjugate, given by $u_m(r,\theta) := w_m(r)\, \mathsf{e}^{\pm \mathrm{i}m\theta}$. It turns out $\mathcal{R}[a_{\mathsf{c}}, R] = \bigcup_{m\in\mathbb{N}} \mathcal{R}[a_{\mathsf{c}}, R](m)$.

The resonances set $(\mathcal{R}[a_{\mathsf{c}}, R](m))_m$ defined in Equation (3.9) cannot be computed analytically, however one can use contour integration techniques on Equation (3.5) to compute a subset $\mathcal{R}_N[a_{\mathsf{c}}, R] := \bigcup_{m=0}^{N} \mathcal{R}[a_{\mathsf{c}}, R](m) \subset \mathcal{R}[a_{\mathsf{c}}, R]$ (see Kravanja & Van Barel (2000); Parini (2018)). Figure 3 represents the set $\mathcal{R}_N[a_{\mathsf{c}}, 1]$, for the unit disk and for various permittivities a_{c}. The colour bar indicates the value of m.

In classical cavities ($a_{\mathsf{c}} > 0$), resonances of Equation (2.3) are split into two categories (at least for $a_{\mathsf{c}} > 1$, Balac *et al.* (2021)): inner resonances $\mathcal{R}_{\mathsf{inn}}[a_{\mathsf{c}}, R]$ associated with resonant modes essentially supported inside the cavity Ω and outer resonances $\mathcal{R}_{\mathsf{out}}[a_{\mathsf{c}}, R]$ associated with resonant modes essentially supported in the exterior of the cavity $\mathbb{R}^2 \setminus \overline{\Omega}$. The inner resonance category includes the so-called WGM, associated with resonances ℓ_{WGM} such that $-1 \ll \Im(\ell_{\mathrm{WGM}}) < 0$ (Cho *et al.*, 2010; Balac *et al.*, 2021). In particular, the approximation of Equation (2.2) can be deteriorated if one chooses $k = \Re(\ell_{\mathrm{WGM}})$, where those modes can be excited (Moiola & Spence, 2019, Section 6.2). When $a_{\mathsf{c}} < 0$ we split the resonances into three categories. From Figs 3 to 5, we conclude:

- The main family of interest represented by '+' in Fig. 3 is associated with resonant modes essentially supported on the interface Γ (see Figs 5 and 6 for an example). We refer to those modes as surface plasmons waves (SPW), and we call this family the interface resonances $\mathcal{R}_{\mathsf{pla}}[a_{\mathsf{c}}, 1]$. We denote the interface resonances $(\ell_m)_{m\geq 1}$ so that $\mathcal{R}_{\mathsf{pla}}[a_{\mathsf{c}}, 1] = \{\ell_m \,|\, m \in \mathbb{N}^*\}$. Observe that the interface resonances' nature changes depending on a_{c}: if $a_{\mathsf{c}} < -1$, then ℓ_m is a resonance close to the positive real axis with $\Re(\ell_m) > 0$ and $-1 \ll \Im(\ell_m) < 0$ (in the ℓ_m plane); if $-1 < a_{\mathsf{c}} < 0$, then $\ell_m \in \mathrm{i}\mathbb{R}_+$ so ℓ_m^2 is a negative eigenvalue.
- The outer resonances $\ell_{\mathsf{out}} \in \mathcal{R}_{\mathsf{out}}[a_{\mathsf{c}}, 1]$ (ℓ_{out} are represented as '•' in Fig. 3) are resonances with a negative imaginary part (in the ℓ_{out} plane). The outer resonant modes are essentially supported outside the cavity (see Figs 5 and 4 for an example).
- The last family (represented as '×' in Fig. 3) corresponds to pure imaginary eigenvalues of the operator P on $\mathrm{L}^2(\mathbb{R}^2)$ (consequently $\ell^2 \in \mathbb{R}_-$). The associated modes are essentially supported inside the cavity (like inner resonant modes, see Figs 5 and 4 for an example). They contain WGM.

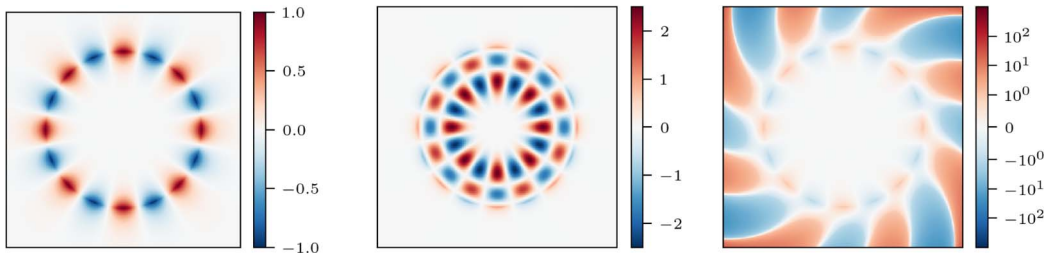

FIG. 5. Real part of some resonant modes $u_8(r,\theta)$ for $a_{\mathsf{c}} = -0.9$ with their corresponding resonances below.

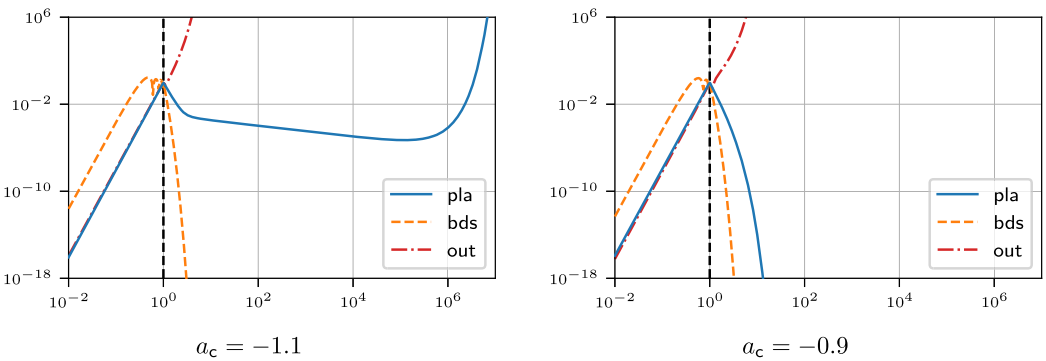

FIG. 6. Log–log plots of the radial component $r \mapsto w_8(r)$ of the three types of resonances shown in Figs 4 and 5 for $a_{\mathsf{c}} = -1.1$ (left) and $a_{\mathsf{c}} = -0.9$ (right).

Because of their particular nature, they are sometimes called bound states (Dyatlov & Zworski, 2019, Chapter 1), and we denote them $\ell_{\mathsf{bds}} \in \mathcal{R}_{\mathsf{bds}}[a_{\mathsf{c}}, 1]$ (consequently $\ell_{\mathsf{bds}}^2 \in \mathbb{R}_-$).

In the end, we write $\mathcal{R}[a_{\mathsf{c}}, R] = \mathcal{R}_{\mathsf{out}}[a_{\mathsf{c}}, R] \cup \mathcal{R}_{\mathsf{bds}}[a_{\mathsf{c}}, R] \cup \mathcal{R}_{\mathsf{pla}}[a_{\mathsf{c}}, R]$. As mentioned before, the interface resonances are quite peculiar as their nature changes depending on a_{c}. As illustrated in Fig. 3, they correspond to complex resonances such that $\Re(\ell_m) > 0$ and $\Im(\ell_m) < 0$ in the ℓ_m plane when $a_{\mathsf{c}} < -1$, while they are pure imaginary eigenvalues $\ell_m \in \mathrm{i}\mathbb{R}_+$ when $-1 < a_{\mathsf{c}} < 0$. For the first case, one observes that $\Re(\ell_m)$ diverges towards $+\infty$ as $m \to \infty$, and their negative imaginary part $\Im(\ell_m) < 0$ tends to 0 exponentially fast as $m \to \infty$. Additionally, a closer observation gives us that $\Re(\ell_m) \propto m$. Figure 6 represents the behaviour of w_8 for the three types of resonances far from the boundary for $a_{\mathsf{c}} \in \{-1.1, -0.9\}$. As discussed above, the support of the bound states and outer resonant modes is mainly inside and outside the cavity, respectively. The modes associated with interface resonances are locally exponentially decreasing moving away from the interface, which is the mathematical characterization of surface plasmons (Maier, 2007; Bonnet-Ben Dhia *et al.*, 2016). In the next section, we characterize to leading order these interface resonances family $(\ell_m)_{m\geq 1}$ by performing asymptotic expansion as $m \to \infty$. In particular, we will confirm that $\Re(\ell_m) \propto m$.

REMARK 3.5. As seen above, it is convenient to identify the change of behaviour of the interface resonances using the sign of $\Re(\ell_m^2)$. In what follows we provide asymptotic expansions of $(\ell_m^2)_{m\geq 1}$ instead of the resonances $(\ell_m)_{m\geq 1}$.

REMARK 3.6. Going back to the Equation (2.2), it turns out that the dashed blue line in Fig. 2 corresponds to the real part an interface resonance: $k_8 = \Re(\ell_8) \approx 2.377$, and $\ell_8 \in \mathcal{R}_{\mathsf{pla}}[-1.1, 1]$. Additionally, given data associated with $k > 0$, the interface modes associated with $\ell \in \mathcal{R}_{\mathsf{pla}}[-0.9, 1]$ (in other words $\Re(\ell^2) < 0$) cannot be excited as illustrated in Fig. 2. One can also perform the same computations for a lossy circular cavity. In that case the interface resonances plunge further into the complex plane (their imaginary part gets more significant in absolute value, moving the resonances away from the real axis). Excitation of those resonances is then more difficult to observe.

3.2 *Interpretation with Schrödinger operator for the disk*

From Section 3.1 we found that plasmonic resonances $(\ell_m)_m$ are such that $\Re(\ell_m^2)$ changes sign depending on a_{c} (*i.e.* η). In this section we use asymptotic expansions to explain this change of behaviour at leading order. To do so, we provide an analogy with the Schrödinger operator. We define $\check{\lambda} = m^{-2}\,\ell^2$, and we rewrite Problem Equation (3.7) as

$$\begin{cases} -m^{-2}\frac{1}{r}\partial_r\big(r\,\partial_r w_m^{\pm}\big) + \dfrac{1}{r^2} w_m^{\pm} = a(r)\,\check{\lambda} w_m^{\pm} & \text{in } (0,R)\cup(R,+\infty) \\ w_m^-(R) = w_m^+(R) \text{ and } -\eta^{-2}\,\partial_r w_m^-(R) = \partial_r w_m^+(R) & \text{across } \{R\} \\ w_0^-(0) = 0 \text{ and } w_m^+ \in \mathscr{S}([R,+\infty)) \end{cases} \tag{3.11}$$

with $\check{\lambda}$ the new spectral parameter, $w_m^{\pm}$ restrictions of w_m in each material and $\mathscr{S}(\mathbb{R}_+)$ denoting the Schwartz space. We replace the outgoing wave condition by the requirement that w_m^+ belongs to the Schwartz space in order to characterize exponentially decreasing behaviours from both sides close to the interface (*i.e.* surface plasmons). To identify this behaviour, first we rescale the problem Equation (3.11) by $\xi = r/R - 1$ such that $r = R$ corresponds to $\xi = 0$. We then define $v_m^{\pm}(\xi) = w_m^{\pm}(R\,(1+\xi))$, satisfying in particular

$$-\,m^{-2}\,\mathscr{L} v_m^{\pm} + V v_m^{\pm} = a(\xi)\,R^2\check{\lambda}\,v_m^{\pm} \qquad \text{in } (-1,0) \text{ and } (0,+\infty),$$

where $\mathscr{L}(\xi,\partial_\xi) = \frac{1}{1+\xi}\partial_\xi((1+\xi)\,\partial_\xi)$ is a positive elliptic operator (Laplacian like) and $V(\xi) = \frac{1}{(1+\xi)^2}$ is a potential. In that sense, the operator $v \mapsto (-m^{-2}\,\mathscr{L} + V)v$ can be interpreted as a Schrödinger operator. To construct localized modes at the interface, we consider the principal part of $-m^{-2}\mathscr{L} + V$ with its coefficients frozen at $\xi = 0$, corresponding to $-m^{-2}\partial_\xi^2 + 1$. It is then natural to rescale by $\rho = m\xi$, and the leading order behaviour becomes

$$\begin{cases} -\partial_\rho^2\varphi^- + \varphi^- = -\eta^2\,R^2\check{\lambda}\,\varphi^- & \text{in } (-\infty,0) \\ -\partial_\rho^2\varphi^+ + \varphi^+ = R^2\check{\lambda}\,\varphi^+ & \text{in } (0,+\infty) \\ \varphi^-(0) = \varphi^+(0) \text{ and } \eta^{-2}\,\partial_\rho\varphi^-(0) = \partial_\rho\varphi^+(0) & \text{across } \{0\}, \\ \varphi^{\pm} \in \mathscr{S}(\mathbb{R}_{\pm}) \end{cases} \tag{3.12}$$

with $\varphi^{\pm}(\rho) = v_m^{\pm}(\xi)$. Note that the condition $v_m^-(-1) = \varphi^-(-m) = 0$ becomes $\varphi^- \in \mathscr{S}(\mathbb{R}_-)$ to keep a localized behaviour as $m \to +\infty$. Solutions of Equation (3.12) are given by $(\check{\lambda}, \varphi^{\pm}) =$

$(R^{-2}(1-\eta^{-2}), \mathsf{e}^{-\eta^{\mp 1}|\rho|})$, where the modes are exponentially decreasing on both sides of the interface $\rho = 0$. Back to Equation (3.11), we have found a pair $(\underline{\lambda}_m, \underline{w}_m^{\pm})$ characterizing $(\ell^2, w_m^{\pm})$, with the leading behaviour given by

$$\underline{\lambda}_m = \frac{m^2}{R^2}\left(1-\eta^{-2}\right) + \mathcal{O}(m), \quad \text{and} \quad \underline{w}_m^{\pm}(r) = \exp\left(-\eta^{\mp 1} m \left|\frac{r}{R} - 1\right|\right) + \mathcal{O}\left(m^{-1}\right). \tag{3.13}$$

We conclude:

- when $a_{\mathsf{c}} < -1$, or $\eta > 1$, SPW are associated with scattering resonances with $\Re(\ell) > 0$ (at first order);
- when $-1 < a_{\mathsf{c}} < 0$, or $0 < \eta < 1$, SPW are associated with negative eigenvalues with $\ell \in \mathrm{i}\mathbb{R}_+$ (at first order).

We have then asymptotically characterized SPW by building pairs $(\underline{\lambda}_m, \underline{w}_m)_{m\geq 1}$. Upon proper justification that $\underline{w}_m(r)e^{\mathrm{i}m\theta} \in \mathcal{D}(P)$ and that $k = \underline{k}_m := \sqrt{\underline{\lambda}_m}$ affects the resolvent, the obtained results match the observed behaviours in previous sections, and provide accurate predictions.

The case of the circular cavity with constant a_{c} is quite intuitive, and the leading order computations can be done explicitly. In the next sections we generalize the approach, to any order, for the general case (arbitrary shaped smooth boundary, and varying coefficients $a_{\mathsf{c}} \in \mathscr{C}^{\infty}(\overline{\Omega}; (-\infty, 0) \setminus \{-1\})$), and justify the connection between the formal expansions (Section 4) and the resolvent operator (as well as the scattering instabilities, consequently) (Section 5). To that aim, we will use semi-classical WKB (Wentzel–Kramers–Brillouin) expansions along the interface and matched asymptotic expansions in the transverse direction to the interface in a tubular neighborhood of the interface. The higher order terms allow to show a super-algebraic behaviour of the peaks seen in Fig. 2, explaining the exponential increase asymptotically.

REMARK 3.7. The circular cavity allows to clearly separate the resonant modes into three categories, where the support is clearly identified. Due to this clear separation, we say that this is a *non-trapping* cavity. A trapping cavity (typically a crescent shape) may allow a combination of localized interface modes with localized outer modes in region encapsulated by the cavity. In the latter, the proposed asymptotic approach may not include the combined modes (the proposed specific scaling above is only adapted for localized plasmonic behaviours). For simplicity, all numerical examples will consider non-trapping cavities, which illustrate the fact that scattering resonances exhibit localized behaviours associated with SPW.

4. Quasi-pair for unbounded transmission problems with sign-changing coefficient

In this section we prove Theorem 2.3 which consists of constructing approximate solutions of the resonance problem in Equation (2.3). Those solutions are called quasi-pairs, in the sense of Definition 2.2. The proof is organized as follows:

- We define a tubular neighborhood where we set up the problem, and we define formal expansions (Section 4.1).
- We compute the expansion terms by solving a family of problems indexed by the order of the expansions (Section 4.2).

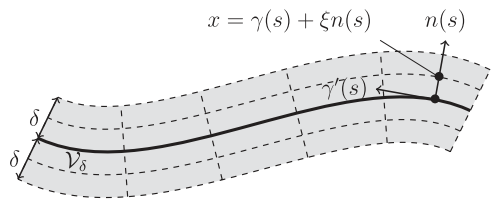

FIG. 7. Tubular neighborhood and notations: s denotes an arc-length parametrization of the curve γ, and ξ is the normal variable.

- We show that the obtained expansions are quasi-pairs in the sense of Definition 2.2 (Lemma 4.9), and that the quasi-resonances are independent of the construction (Corollary 4.13). Details are given in Section 4.3.

We end Section 4 with comments on the first expansion terms of $\left(\underline{\lambda}_m\right)_{m\geq 1}$.

4.1 *Formal expansion set-up*

Recall that $\Omega \subset \mathbb{R}^2$ is a cavity with smooth boundary Γ, see Section 2.1. Let L be the length of Γ, and $\eta := \sqrt{-a_{\mathsf{c}}}$ a positive smooth function up to the interface so that we have $a_{\mathsf{c}} = -\eta^2$. We define a tubular neighborhood $\mathcal{V}_\delta$ of the interface Γ. Let $\gamma : \mathbb{T}_L \to \Gamma$ be a counterclockwise curvilinear parametrization of the curve Γ with the notation $\mathbb{T}_L := \mathbb{R}/L\mathbb{Z}$. Let $n = (\gamma_2', -\gamma_1')^{\mathsf{T}}$ be the unit exterior normal to Ω and $\kappa = \det\left(\gamma', \gamma''\right) : \mathbb{T}_L \to \mathbb{R}$ be the signed curvature. We define the open tubular neighborhood, see Moon & Spencer (1988), by

$$\mathcal{V}_\delta := \{\gamma(s) + \xi n(s) \,|\, (s,\xi) \in \mathbb{T}_L \times (-\delta, \delta)\}, \tag{4.1}$$

which is schematically represented in Fig. 7.

We now consider the problem

$$\begin{cases} Pu = \lambda u & \text{in } \Omega \cap \mathcal{V}_\delta \text{ and } \left(\mathbb{R}^2 \setminus \overline{\Omega}\right) \cap \mathcal{V}_\delta \\ [u]_\Gamma = 0 \text{ and } [a^{-1}\,\partial_n u]_\Gamma = 0 & \text{across } \Gamma, \\ u = 0 & \text{on } \partial\mathcal{V}_\delta \end{cases} \tag{4.2}$$

where $P = -\mathrm{div}(a^{-1}\,\nabla)$ with a defined in Equation (2.1). By Definition 2.2, the quasi-pairs are compactly supported therefore the outgoing condition does not play a role in their construction. We replace in particular the outgoing wave condition by a homogeneous Dirichlet boundary condition in order to construct localized quasi-pairs.

The change of variables from the tubular coordinates $(s,\xi) \in \mathbb{T}_L \times (-\delta,\delta)$ to the Cartesian coordinates $x \in \mathcal{V}_\delta$ is a smooth diffeomorphism for $0 < \delta < (\max_{\mathbb{T}_L} |\kappa|)^{-1}$. In this tubular coordinate system the operator P becomes

$$P = -g^{-1}\,\mathrm{div}_{s,\xi}\left(a^{-1}\,G\,\nabla_{s,\xi}\right), \tag{4.3}$$

where $g(s,\xi) = 1 + \xi\kappa(s) > 0$ and $G(s,\xi) = \begin{pmatrix} g(s,\xi)^{-1} & 0 \\ 0 & g(s,\xi) \end{pmatrix}$.

For the general case, we use a WKB framework (Babič & Buldyrev, 1991) in order to provide an asymptotic expansion of the spectral parameter as the number of oscillations along the interface Γ, denoted m in Section 3.2, goes to infinity. We introduce a small parameter $h > 0$ (later to be linked to m) and the ansatz for the quasi-pair (λ, u):

$$u(s,\xi) = w(s,\xi)\, \exp\left(\tfrac{\mathrm{i}}{h}\,\theta(s)\right) \quad \text{and} \quad \lambda = h^{-2}\,\breve{\lambda}, \tag{4.4}$$

where $\frac{1}{h}\theta\colon [0,L] \to \mathbb{C}$ is the fast phase along the interface, $w\colon \mathbb{T}_L \times (-\delta,\delta) \to \mathbb{C}$ is the slow amplitude and $\breve{\lambda} \in \mathbb{C}$ is the spectral parameter. In order for the function u in Equation (4.4) to be a smooth function in $\mathcal{V}_\delta \setminus \Gamma$, we need to add the constraint that the function $s \mapsto \mathsf{e}^{\frac{\mathrm{i}}{h}\theta(s)} \in \mathscr{C}^\infty(\mathbb{T}_L)$. The phase function is chosen to be complex to simplify the computations, however we can always put the imaginary part into the amplitude w. Following Babič & Buldyrev (1991), we formally expand the unknowns w, θ and $\breve{\lambda}$ with respect to h as

$$w(s,\xi) = \sum_{n\geq 0} w_n(s,\xi)\, h^n, \quad \theta(s) = \sum_{n\geq 0} \theta_n(s)\, h^n \quad \text{and} \quad \breve{\lambda} = \sum_{n\geq 0} \breve{\lambda}_n\, h^n. \tag{4.5}$$

The system Equation (4.2) with the new unknowns in Equation (4.4) becomes

$$\begin{cases} \mathcal{L}_h[a](w,\theta) = \breve{\lambda}\, w & \text{in } \mathbb{T}_L \times [(-\delta,0)\cup(0,\delta)] \\ [w]_{\mathbb{T}_L\times\{0\}} = 0 \text{ and } [a^{-1}\,\partial_\xi w]_{\mathbb{T}_L\times\{0\}} = 0 & \text{across } \mathbb{T}_L \times \{0\} \\ w = 0 & \text{on } \mathbb{T}_L \times \{-\delta,\delta\} \end{cases}. \tag{4.6}$$

Above, $\mathcal{L}_h[a](w,\theta) = h^2\, \mathsf{e}^{-\frac{\mathrm{i}}{h}\theta}\, P\left(w\, \mathsf{e}^{\frac{\mathrm{i}}{h}\theta}\right)$, and it can be decomposed as

$$\mathcal{L}_h[a](w,\theta) = \mathcal{L}_h^3[a](w,\theta,\theta) + \mathcal{L}_h^2[a](w,\theta) + \mathcal{L}_h^1[a](w), \tag{4.7}$$

where $\mathcal{L}_h^j[a]$ are j-linear for $j \in \{1,2,3\}$ and

$$\mathcal{L}_h^3[a](w,\theta,\vartheta) = g^{-2}\, a^{-1}\, w\, \partial_s\theta\, \partial_s\vartheta, \tag{4.8a}$$

$$\mathcal{L}_h^2[a](w,\theta) = -h\,\mathsf{i}\left(g^{-2}\, a^{-1}\, \partial_s w\, \partial_s\theta + g^{-1}\, \partial_s\left(g^{-1}\, a^{-1}\, w\, \partial_s\theta\right)\right), \tag{4.8b}$$

$$\mathcal{L}_h^1[a](w) = -h^2\, g^{-1}\left(\partial_\xi\left(g\, a^{-1}\, \partial_\xi w\right) + \partial_s\left(g^{-1}\, a^{-1}\, \partial_s w\right)\right). \tag{4.8c}$$

In the above decomposition, only $\mathcal{L}_h^1[a]$ involves derivatives with respect to ξ. Since g (resp. $\eta = \sqrt{-a_{\mathsf{c}}} > 0$) is a smooth function on $\mathbb{T}_L \times (-\delta,\delta)$ (resp. $\mathbb{T}_L \times (-\delta,0]$), then G is smooth, and we write

the formal Taylor expansions at $\xi = 0$:

$$g(s,\xi) = 1 + \xi\kappa(s), \quad G(s,\xi) = \sum_{n\geq 0} \frac{\partial_\xi^n G(s,0)}{n!}\,\xi^n, \quad \eta(s,\xi) = \sum_{n\geq 0} \frac{\eta_n(s)}{n!}\,\xi^n, \tag{4.9}$$

where $\eta_n(s) = \partial_\xi^n \eta(s,0)$. Since g and η do not vanish on $\mathbb{T}_L \times \{0\}$, the formal expansions of g^{-1}, g^{-2} and η^{-2} about $\xi = 0$ can be computed with Equation (4.9).

Like in Section 3.2, we introduce the scaled variable $\rho = h^{-1}\xi$ for the normal variable $\xi \in (-\delta, \delta)$, and we define

$$\varphi^\pm(s,\rho) = w(s,h\rho), \qquad \text{for } (s,\rho) \in \mathbb{T}_L \times \mathbb{R}_\pm.$$

Then, with $g = g(s,h\rho)$ we rewrite

$$\mathcal{L}_h^1[a](\varphi^\pm) = -g^{-1}\,\partial_\rho\Big(a^{-1}\,g\,\partial_\rho\varphi^\pm\Big) - h^2\,g^{-1}\,\partial_s\Big(a^{-1}\,g^{-1}\,\partial_s\varphi^\pm\Big). \tag{4.10}$$

Equation (4.6) becomes the formal problem: Find $(\varphi_n^\pm)_{n\in\mathbb{N}} \in \mathscr{C}^\infty(\mathbb{T}_L, \mathscr{S}(\mathbb{R}_\pm))^{\mathbb{N}}$, $\Big(\exp(\frac{\mathrm{i}}{h}\theta_n)\Big)_{n\in\mathbb{N}} \in \mathscr{C}^\infty(\mathbb{T}_L)^{\mathbb{N}}$, and $(\check{\lambda}_n)_{n\in\mathbb{N}} \in \mathbb{C}^{\mathbb{N}}$ such that

$$\begin{cases} \mathcal{L}_h[a]\big(\sum_n \varphi_n^\pm\, h^n, \sum_n \theta_n\, h^n\big) = \big(\sum_n \check{\lambda}_n\, h^n\big)\big(\sum_n \varphi_n^\pm\, h^n\big) & \text{in } \mathbb{T}_L \times \mathbb{R}_\pm^* \\ \sum_n \varphi_n^-(s,0)\, h^n = \sum_n \varphi_n^+(s,0)\, h^n & \text{on } \mathbb{T}_L \times \{0\}\,. \\ -\eta_0(s)^{-2}\,\sum_n \partial_\rho\varphi_n^-(s,0)\, h^n = \sum_n \partial_\rho\varphi_n^+(s,0)\, h^n & \text{on } \mathbb{T}_L \times \{0\} \end{cases} \tag{4.11}$$

Note that for simplicity we extend the scaled domain $\mathbb{T}_L \times (-\frac{\delta}{h}, \frac{\delta}{h})$ to the domain $\mathbb{T}_L \times \mathbb{R}$ in order to be independent of h in Equation (4.11), and we replace the homogeneous Dirichlet boundary condition on $\mathbb{T}_L \times \{-\frac{\delta}{h}, \frac{\delta}{h}\}$ by the conditions $\rho \mapsto \varphi^\pm(s,\rho) \in \mathscr{S}(\mathbb{R}_\pm)$ for all $s \in \mathbb{T}_L$. One can always multiply the quasi-mode by a cut-off function $\xi \mapsto \chi(\xi)$ to be in the domain $\mathbb{T}_L \times (-\frac{\delta}{h}, \frac{\delta}{h})$, as done later in Equation (4.16). With Equation (4.7) and Equation (4.9), we can formally expand the operators $\mathcal{L}_h^j[-\eta^2] = \sum_{n\geq 0} \mathsf{L}_n^{j,-}\, h^n$ and $\mathcal{L}_h^j[1] = \sum_{n\geq 0} \mathsf{L}_n^{j,+}\, h^n$, where $\mathsf{L}_n^{j,\pm}$ are independent of h, for $j \in \{1,2,3\}$. From Problem Equation (4.11), we obtain the family of problems $(\mathcal{P}_n)_{n\in\mathbb{N}}$ by identifying powers of h: Find $\varphi_n^\pm \in \mathscr{C}^\infty(\mathbb{T}_L, \mathscr{S}(\mathbb{R}_\pm))$, $\exp(\frac{\mathrm{i}}{h}\theta_n) \in \mathscr{C}^\infty(\mathbb{T}_L)$, and $\check{\lambda}_n \in \mathbb{C}$ such that

$$\begin{cases} \displaystyle\sum_{p\in\mathbb{N}_n^4} \mathsf{L}_{p_1}^{3,\pm}\Big(\varphi_{p_2}^\pm, \theta_{p_3}, \theta_{p_4}\Big) + \sum_{p\in\mathbb{N}_n^3} \mathsf{L}_{p_1}^{2,\pm}\Big(\varphi_{p_2}^\pm, \theta_{p_3}\Big) + \sum_{p\in\mathbb{N}_n^2} \mathsf{L}_{p_1}^{1,\pm}\Big(\varphi_{p_2}^\pm\Big) = \sum_{p\in\mathbb{N}_n^2} \check{\lambda}_{p_1}\,\varphi_{p_2}^\pm \\ \varphi_n^-(s,0) = \varphi_n^+(s,0) \quad \text{and} \quad -\eta_0(s)^{-2}\,\partial_\rho\varphi_n^-(s,0) = \partial_\rho\varphi_n^+(s,0) \end{cases} \tag{4.12}$$

with the notation $\mathbb{N}_n^d = \{p \in \mathbb{N}^d \mid p_1 + \cdots + p_d = n\}$.

4.2 *Computation of the expansion terms*

First, we set some notation that will be useful throughout the rest of the section.

NOTATION 4.1. We recall that $\eta_0 = \eta|_\Gamma = \sqrt{-a_{\mathsf{c}}|_\Gamma}$. Since we assume that $1 + a_{\mathsf{c}}|_\Gamma^{-1} = 1 - \eta_0^{-2} \neq 0$, we can define the scalar $\varsigma = \pm 1$ to be the sign of $1 - \eta_0^{-2}$, the functions $\tau_0 = |1 - \eta_0^{-2}|^{-\frac{1}{2}}$, and $\widehat{\tau}_0 = \frac{\tau_0}{\langle \tau_0 \rangle}$ where $\langle \cdot \rangle$ is the mean along the interface Γ defined by

$$\langle f \rangle := \frac{1}{L} \int_{\mathbb{T}_L} f(s) \mathrm{d}s, \qquad \forall f \in \mathrm{L}^1(\mathbb{T}_L).$$

One can obtain the expressions for the $\mathsf{L}_0^{j,\pm}$.

LEMMA 4.2. The first terms of the expansions of $\mathcal{L}_h^3[a]$, $\mathcal{L}_h^2[a]$ and $\mathcal{L}_h^1[a]$ are given by

$$\begin{aligned}
&\mathsf{L}_0^{3,-}(\phi,\theta,\vartheta) = -\eta_0^{-2}\,\phi\,\partial_s\theta\,\partial_s\vartheta, && \mathsf{L}_0^{2,-}(\phi,\theta) = 0, && \mathsf{L}_0^{1,-}(\phi) = \eta_0^{-2}\,\partial_\rho^2\phi,\\
&\mathsf{L}_0^{3,+}(\phi,\theta,\vartheta) = \phi\,\partial_s\theta\,\partial_s\vartheta, && \mathsf{L}_0^{2,+}(\phi,\theta) = 0, && \mathsf{L}_0^{1,+}(\phi) = -\partial_\rho^2\phi.
\end{aligned}$$

Proof. From the expressions (4.8a), (4.8b) and (4.10) and using the expansions (4.9) with the change of variable $\xi = h\rho$ gives the expressions in the lemma. □

Using Lemma 4.2, we rewrite Problem $(\mathcal{P}_0)$ as: Find $\varphi_0^\pm \in \mathscr{C}^\infty(\mathbb{T}_L, \mathscr{S}(\mathbb{R}_\pm))$, $\theta_0 \in \mathscr{C}^\infty([0,L])$, and $\check{\lambda}_0 \in \mathbb{C}$ such that $(\varphi_0^-, \varphi_0^+) \not\equiv (0,0)$, $\exp(\frac{\mathrm{i}}{h}\theta_0) \in \mathscr{C}^\infty(\mathbb{T}_L)$, and

$$\begin{cases}
\partial_\rho^2\varphi_0^- - \left(\theta_0'^2 + \eta_0^2\,\check{\lambda}_0\right)\varphi_0^- = 0 & \text{in } \mathbb{T}_L \times \mathbb{R}_-\\
\partial_\rho^2\varphi_0^+ - \left(\theta_0'^2 - \check{\lambda}_0\right)\varphi_0^+ = 0 & \text{in } \mathbb{T}_L \times \mathbb{R}_+\\
\varphi_0^-(s,0) = \varphi_0^+(s,0) & \text{on } \mathbb{T}_L \times \{0\}\\
-\eta_0(s)^{-2}\,\partial_\rho\varphi_0^-(s,0) = \partial_\rho\varphi_0^+(s,0) & \text{on } \mathbb{T}_L \times \{0\}
\end{cases}. \tag{4.13}$$

LEMMA 4.3. One can choose $h = \frac{L}{2\pi m}$ for $m \in \mathbb{N}^*$ so that $(\varphi_0^\pm, \theta_0, \check{\lambda}_0)$ is given by

$$\check{\lambda}_0 = \frac{\varsigma}{\langle \tau_0 \rangle^2}, \quad \theta_0(s) = \int_0^s \widehat{\tau}_0(t)\mathrm{d}t, \quad \text{and} \quad \varphi_0^\pm(s,\rho) = \alpha(s)\exp\left(-|\rho|\,\widehat{\tau}_0(s)\,\eta_0(s)^{\mp 1}\right),$$

with $\alpha \in \mathscr{C}^\infty(\mathbb{T}_L, \mathbb{C}^*)$ (and ς, τ_0 defined in Notation 4.1), is solution of Problem $(\mathcal{P}_0)$ defined in Equation (4.13).

The proof is detailed in Appendix B.1.

REMARK 4.4.

- If we unravel the scaling and return to tubular coordinates, for $m \geq 1$ and $(s,\xi) \in \mathbb{T}_L \times \mathbb{R}$, we formally have a pair $(\underline{\lambda}_m, \underline{u}_m)$

$$\underline{\lambda}_m = \left(\frac{2\pi m}{L}\right)^2 \left[\check{\lambda}_0 + \mathcal{O}\left(m^{-1}\right)\right],$$

$$\underline{u}_m(s,\xi) = \mathsf{e}^{\mathsf{i}\frac{2\pi m}{L}[\theta_0(s)+\mathcal{O}(m^{-1})]} \begin{cases} \varphi_0^-\left(s, \frac{2\pi m}{L}\xi\right), & \text{if } \xi \leq 0 \\ \varphi_0^+\left(s, \frac{2\pi m}{L}\xi\right), & \text{if } \xi > 0 \end{cases} + \mathcal{O}\left(m^{-1}\right),$$

  which characterizes surface plasmons at leading order.

- We remark that the leading order term, solution of Equation (4.13), can be seen as the leading order solution of a planar problem of the form $-\mathrm{div}(a^{-1}\nabla\tilde{u})$ on $\mathbb{T}_L \times \mathbb{R}$ with $a(s,y) = -\eta_0^2$ on the lower half-plane, $a \equiv 1$ on the upper half-plane, and $\nu \in \mathbb{R}$.

REMARK 4.5. The construction relies on several choices that are not unique.

- One can choose the main phase to satisfy $\theta_0' = \widehat{\tau}_0$ or $\theta_0' = -\widehat{\tau}_0$. Then one can construct two modes corresponding to $\underline{u}_m$ and $\overline{\underline{u}_m}$ (see Remark 4.14), where $\overline{\cdot}$ is the complex conjugate.
- The function θ_0 is defined up to a constant c. Then $\underline{u}_m$ in Remark 4.4 is defined up to $\mathsf{e}^{\mathsf{i}\frac{2\pi m}{L}c}$. For simplicity, we consider $c = 0$ as we normalize in the end.
- The functions $\varphi_0^\pm$ are defined up to a function $\alpha\colon \mathbb{T}_L \to \mathbb{C}^*$, which contributes to the phase of $\underline{u}_m$ and therefore affects the number of oscillations along the interface. One can always shift indices so that $(\underline{\lambda}_m, \underline{u}_m)_{m \geq 1-q_\alpha}$, for some $q_\alpha \in \mathbb{Z}$, corresponds to a wave with m oscillations along the interface.
- We choose $h = \frac{L}{2\pi m}$ to simplify the computations; however, other choices can be made, as long as we have $h \propto m^{-1}$.

Now, to compute the higher order term of the expansion, from Equation (4.12), Lemma 4.2 and Lemma 4.3, for $n \geq 1$, we can rewrite Problem $(\mathcal{P}_n)$ as: Find $\varphi_n^\pm \in \mathscr{C}^\infty(\mathbb{T}_L, \mathscr{S}(\mathbb{R}_\pm))$, $\exp(\mathsf{i}\, h^{n-1}\theta_n) \in \mathscr{C}^\infty(\mathbb{T}_L)$, and $\check{\lambda}_n \in \mathbb{C}$ such that

$$\begin{cases} \partial_\rho^2 \varphi_n^- - \widehat{\tau}_0^2\, \eta_0^2\, \varphi_n^- = \left(2\widehat{\tau}_0\, \theta_n' + \eta_0^2\, \check{\lambda}_n\right)\varphi_0^- + \eta_0^2\, S_{n-1}^- & \text{in } \mathbb{T}_L \times \mathbb{R}_- \\ \partial_\rho^2 \varphi_n^+ - \widehat{\tau}_0^2\, \eta_0^{-2}\, \varphi_n^+ = \left(2\widehat{\tau}_0\, \theta_n' - \check{\lambda}_n\right)\varphi_0^+ - S_{n-1}^+ & \text{in } \mathbb{T}_L \times \mathbb{R}_+ \\ \varphi_n^-(s,0) = \varphi_n^+(s,0) & \text{on } \mathbb{T}_L \times \{0\}, \\ -\eta_0(s)^{-2}\, \partial_\rho \varphi_n^-(s,0) = \partial_\rho \varphi_n^+(s,0) & \text{on } \mathbb{T}_L \times \{0\} \end{cases} \tag{4.14}$$

where

$$S_{n-1}^{\pm} = \sum_{p=1}^{n-1} \breve{\lambda}_{n-p}\, \varphi_p^{\pm} - \sum_{p=0}^{n-1} \mathsf{L}_{n-p}^{1,\pm}\left(\varphi_p^{\pm}\right) - \sum_{p\in\mathbb{I}_n^3} \mathsf{L}_{p_1}^{2,\pm}\left(\varphi_{p_2}^{\pm}, \theta_{p_3}\right)$$
$$- \mathsf{L}_n^{2,\pm}\left(\varphi_0^{\pm}, \theta_0\right) - \sum_{p\in\mathbb{I}_n^4} \mathsf{L}_{p_1}^{3,\pm}\left(\varphi_{p_2}^{\pm}, \theta_{p_3}, \theta_{p_4}\right) - \mathsf{L}_n^{3,\pm}\left(\varphi_0^{\pm}, \theta_0, \theta_0\right) \tag{4.15}$$

with $\mathbb{I}_n^d = \{p \in [\![0, n-1]\!]^d \,|\, p_1 + \cdots + p_d = n\}$.

LEMMA 4.6. Define $(\varphi_0^{\pm}, \theta_0, \breve{\lambda}_0)$ according to Lemma 4.3. For $n \geq 1$, there exists a solution $(\varphi_n^{\pm}, \theta_n, \breve{\lambda}_n) \in \mathscr{C}^\infty(\mathbb{T}_L, \mathscr{S}(\mathbb{R}_\pm)) \times \mathscr{C}^\infty(\mathbb{T}_L) \times \mathbb{C}$ of Problem $(\mathcal{P}_n)$ defined in Equation (4.14). In particular, $\varphi_n^{\pm}$ is given by

$$\varphi_n^{\pm}(s,\rho) = P_n^{\pm}(s,\rho) \exp\left(-|\rho|\, \widehat{\tau}_0(s)\, \eta_0(s)^{\mp 1}\right),$$

with polynomials $P_n^{\pm} \in \mathscr{C}^\infty(\mathbb{T}_L, \mathbb{P})$[4] .

The proof is detailed in Appendix B.2.

REMARK 4.7. In addition to Remark 4.5, $(\theta_n)_{n\geq 0}$ and $(\varphi_n)_{n\geq 0}$ are not uniquely defined at each step of the construction. However, the sequence $(\breve{\lambda}_n)_{n\geq 0}$ will be unique (see Corollary 4.13).

4.3 *Proof of the Theorem 2.3*

Based on formal series $\sum_n \varphi_n^{\pm} h^n$, $\sum_n \theta_n h^n$ and $\sum_n \breve{\lambda}_n h^n$ with $h = \frac{L}{2\pi m}$, we now construct quasi-pairs in the sense of Definition 2.2. This step is necessary to justify that our formal expansions capture scattering resonances. First we use Borel's Lemma (Hörmander, 2003, Theorem 1.2.6) for $\breve{\lambda}$ and θ, and a direct generalization on the Fréchet space $\mathscr{C}^\infty(\mathbb{T}_L, \mathscr{S}(\mathbb{R}_\pm))$ (Balac *et al.*, 2021, Lemma A.5) for $\varphi^{\pm}$ to establish:

LEMMA 4.8. There exist $\Phi^{\pm} \in \mathscr{C}^\infty([0, \frac{L}{2\pi}] \times \mathbb{T}_L, \mathscr{S}(\mathbb{R}_\pm))$, $\Theta \in \mathscr{C}^\infty([0, \frac{L}{2\pi}] \times \mathbb{T}_L)$, and $\Lambda \in \mathscr{C}^\infty([0, \frac{L}{2\pi}])$ such that, for $N \geq 1$, $h \in [0, \frac{L}{2\pi}]$, $s \in \mathbb{T}_L$, and $\rho \in \mathbb{R}_\pm$, we have

$$\Phi^{\pm}(h; s, \rho) = \sum_{n=0}^{N-1} \varphi_n^{\pm}(s,\rho)\, h^n + h^N R_N^{\pm}(h; s, \rho)$$
$$\Theta(h; s) = \sum_{n=0}^{N-1} \theta_n(s)\, h^n + h^N R_N^{\Theta}(h; s)$$
$$\Lambda(h) = \sum_{n=0}^{N-1} \breve{\lambda}_n\, h^n + h^N R_N^{\Lambda}(h)$$

[4] We denote by $\mathbb{P}$ the space of polynomial of a single variable with complex coefficients.

where $R_N^{\pm} \in \mathscr{C}^\infty([0, \frac{L}{2\pi}] \times \mathbb{T}_L, \mathscr{S}(\mathbb{R}_\pm))$, $R_N^{\Theta} \in \mathscr{C}^\infty([0, \frac{L}{2\pi}] \times \mathbb{T}_L)$, $R_N^{\Lambda} \in \mathscr{C}^\infty([0, \frac{L}{2\pi}])$.

From those functions, we now define the scalars $\underline{\lambda}_m$ and the functions $\underline{u}_m$ in the tubular neighborhood as

$$\underline{\lambda}_m = \left(\tfrac{2\pi m}{L}\right)^2 \Lambda\left(\tfrac{L}{2\pi m}\right) = \left(\tfrac{2\pi m}{L}\right)^2 \sum_{n\in\mathbb{N}} \check{\lambda}_n \left(\frac{L}{2\pi m}\right)^n \tag{4.16a}$$

$$\underline{u}_m(s,\xi) = \chi(\xi)\, \exp\left(\mathrm{i}\tfrac{2\pi m}{L}\, \Theta\left(\tfrac{L}{2\pi m}; s\right)\right) \begin{cases} \Phi^-\left(\tfrac{L}{2\pi m}; s, \tfrac{2\pi m}{L}\xi\right), & \text{if } \xi \le 0 \\ \Phi^+\left(\tfrac{L}{2\pi m}; s, \tfrac{2\pi m}{L}\xi\right), & \text{if } \xi > 0 \end{cases}, \tag{4.16b}$$

where χ is a cutoff function, $\chi \in \mathscr{C}^\infty_{\mathrm{comp}}((-\delta, \delta))$ and $\chi \equiv 1$ on $[-\frac{\delta}{2}, \frac{\delta}{2}]$. In what follows, we establish that Equation (4.16) is a quasi-pair. First we have:

LEMMA 4.9. The pair $(\underline{\lambda}_m, \underline{u}_m)_{m\ge1}$ defined in Equation (4.16) satisfies the following:

(i) $\underline{u}_m$ is uniformly compactly supported and smooth in Ω and $\mathbb{R}^2 \setminus \overline{\Omega}$.

(ii) $\underline{u}_m$ satisfies $[\underline{u}_m]_\Gamma = \mathcal{O}(m^{-\infty})$ and $[a^{-1}\, \partial_n \underline{u}_m]_\Gamma = \mathcal{O}(m^{-\infty})$.

(iii) $\underline{u}_m$ admits the norm expansion

$$\|\underline{u}_m\|_{\mathrm{L}^2(\mathbb{R}^2)} = b\, m^{-\frac{1}{2}} + \mathcal{O}\left(m^{-\frac{3}{2}}\right) \qquad \text{with } b > 0.$$

(iv) Let $\underline{R}_m := P\underline{u}_m - \underline{\lambda}_m\, \underline{u}_m$ be the reminder defined in Ω and $\mathbb{R}^2 \setminus \overline{\Omega}$, then we have

$$\|\underline{R}_m\|_{\mathrm{L}^2(\Omega)} + \|\underline{R}_m\|_{\mathrm{L}^2(\mathbb{R}^2\setminus\overline{\Omega})} = \mathcal{O}(m^{-\infty}).$$

(v) If two quasi-pairs $(\underline{\lambda}_m, \underline{u}_m)_{m\ge1}$, $(\underline{\mu}_m, \underline{v}_m)_{m\ge1}$ satisfy (i)–(iv), and the quasi-modes have the same leading phase $\theta_0(s) = \int_0^s \widehat{\tau}_0(t)\mathrm{d}t$ then:

$$\int_{\mathbb{R}^2} \underline{u}_m\, \overline{\underline{v}_m}\mathrm{d}x = z_0\, m^{-1} + \mathcal{O}\left(m^{-2}\right) \quad \text{and} \quad \int_{\mathbb{R}^2} \underline{u}_m\, \underline{v}_m \mathrm{d}x = \mathcal{O}(m^{-\infty})$$

with $z_0 \in \mathbb{C}^*$.

REMARK 4.10. Items *(iii)* and *(v)* of Lemma 4.9 give us

$$\int_{\mathbb{R}^2} \frac{\underline{u}_m}{\|\underline{u}_m\|_{\mathrm{L}^2(\mathbb{R}^2)}} \frac{\overline{\underline{v}_m}}{\|\overline{\underline{v}_m}\|_{\mathrm{L}^2(\mathbb{R}^2)}} \mathrm{d}x = z_0' + \mathcal{O}\left(m^{-1}\right), \quad \text{with } z_0' \in \mathbb{C}^*.$$

REMARK 4.11. At this point $\underline{u}_m \notin \mathcal{D}(P)$ because the transmission conditions are not exactly satisfied, therefore it is not yet a quasi-pair in the sense of Definition 2.2.

Proof. Proof of Lemma 4.9. Recall that we set $h = \frac{L}{2\pi m}$, and to simplify notations we denote $\chi_h \colon \rho \mapsto \chi(\rho h)$, $\Phi_h^{\pm} \colon (s,\rho) \mapsto \Phi^{\pm}(h;s,\rho)$, $\Theta_h \colon s \mapsto \Theta(h;s)$, and $\Lambda_h = \Lambda(h)$.

(i) By definition of $(\underline{u}_m)_{m\geq 1}$ in Equation (4.16b), *(i)* is satisfied.

(ii) Using Lemma 4.8 and that each functions $\varphi_n^{\pm}$ satisfies the transmission conditions via Lemma 4.6, one can show that $[\underline{u}_m]_\Gamma = \mathcal{O}(m^{-N})$ and $[a^{-1}\,\partial_n \underline{u}_m]_\Gamma = \mathcal{O}(m^{-N})$ for all $N \geq 0$, which is the definition of $\mathcal{O}(m^{-\infty})$.

(iii) We introduce the weighted L^2 semi-norm on $\mathbb{T}_L \times \mathbb{R}_\pm$

$$\|f\|^2_{\mathrm{L}^2_\pm[h]} = \int_{\mathbb{T}_L} \int_{\mathbb{R}_\pm \cap \left(-\frac{\delta}{h}, \frac{\delta}{h}\right)} |f(s,\rho)|^2 \, h(1+\kappa(s)\rho h)\mathrm{d}\rho\mathrm{d}s. \tag{4.17}$$

From Equation (4.16), we obtain

$$\|\underline{u}_m\|^2_{\mathrm{L}^2(\mathbb{R}^2)} = \|\chi_h \Phi_h^- \mathrm{e}^{\frac{\mathrm{i}}{h}\Theta_h}\|^2_{\mathrm{L}^2_-[h]} + \|\chi_h \Phi_h^+ \mathrm{e}^{\frac{\mathrm{i}}{h}\Theta_h}\|^2_{\mathrm{L}^2_+[h]}.$$

From Lemma 4.3 and Lemma 4.8 for $N = 1$, we have

$$\begin{aligned}
\Theta_h(s) &= \int_0^s \widehat{\tau}_0(t)\mathrm{d}t + \theta_1(s)h + h^2 R_2^{\Theta}(h;s) \\
\Phi_h^{\pm}(s,\rho) &= \alpha(s)\, \exp\left(-|\rho|\,\widehat{\tau}_0(s)\,\eta_0(s)^{\mp 1}\right) + h\, R_1^{\pm}(h;s,\rho),
\end{aligned}$$

where $R_2^{\Theta} \in \mathscr{C}^\infty([0, \frac{L}{2\pi}] \times \mathbb{T}_L)$ and $R_1^{\pm} \in \mathscr{C}^\infty([0, \frac{L}{2\pi}] \times \mathbb{T}_L, \mathscr{S}(\mathbb{R}_\pm))$. We deduce that

$$\left| \left\| \chi_h \Phi_h^{\pm} \mathrm{e}^{\frac{\mathrm{i}}{h}\Theta_h} \right\|^2_{\mathrm{L}^2_\pm[h]} - \left\| \chi_h\, \alpha\, \mathrm{e}^{-|\rho|\,\widehat{\tau}_0 \eta_0^{\mp 1}} \mathrm{e}^{\mathrm{i}\,\theta_1} \right\|^2_{\mathrm{L}^2_\pm[h]} \right| \leq C_1^{\pm} h^2$$

for $C_1^{\pm}$ some positive constant. We write $\|\chi_h\, \alpha\, \mathrm{e}^{-|\rho|\,\widehat{\tau}_0 \eta_0^{\mp 1}} \mathrm{e}^{\mathrm{i}\,\theta_1}\|^2_{\mathrm{L}^2_\pm[h]} = I_1^{\pm} + I_2^{\pm} + I_3^{\pm}$,

$$\begin{aligned}
I_1^{\pm} &= h \int_{\mathbb{T}_L} \int_{\mathbb{R}_\pm} |\alpha(s)|^2 \mathrm{e}^{\mp 2\rho\, \widehat{\tau}_0(s)\eta_0(s)^{\mp 1}} \mathrm{e}^{-2\Im(\theta_1(s))} \mathrm{d}\rho\mathrm{d}s = h \int_{\mathbb{T}_L} \frac{|\alpha(s)|^2 \mathrm{e}^{-2\Im(\theta_1(s))}}{2\widehat{\tau}_0(s)\eta_0(s)^{\mp 1}} \mathrm{d}s, \\
I_2^{\pm} &= h \int_{\mathbb{T}_L} \int_{\mathbb{R}_\pm} (|\chi(\rho h)|^2 - 1)|\alpha(s)|^2 \mathrm{e}^{\mp 2\rho\, \widehat{\tau}_0(s)\eta_0(s)^{\mp 1}} \mathrm{e}^{-2\Im(\theta_1(s))} \mathrm{d}\rho\mathrm{d}s, \\
I_3^{\pm} &= h^2 \int_{\mathbb{T}_L} \int_{\mathbb{R}_\pm} |\chi(\rho h)\alpha(s)|^2 \mathrm{e}^{\mp 2\rho\, \widehat{\tau}_0(s)\eta_0(s)^{\mp 1}} \mathrm{e}^{-2\Im(\theta_1(s))}\, \kappa(s)\rho \mathrm{d}\rho\mathrm{d}s.
\end{aligned}$$

One can show that $I_2^{\pm} = \mathcal{O}(h^\infty)$ using Lemma B.1. Since χ is bounded and the function $(h;s,\rho) \mapsto |\alpha|^2 \mathrm{e}^{\mp 2\rho\, \widehat{\tau}_0 \eta_0^{\mp 1}} \mathrm{e}^{-2\Im(\theta_1)} \kappa\rho$ is in $\mathscr{C}^\infty([0, \frac{L}{2\pi}] \times \mathbb{T}_L, \mathscr{S}(\mathbb{R}_\pm))$ there exists a constant $C_3^{\pm}$ such that $|I_3^{\pm}| \leq$

$C_3^{\pm} h^2$. Combining the results we get

$$\|\underline{u}_m\|^2_{\mathrm{L}^2(\mathbb{R}^2)} = b^2\, m^{-1} + \mathcal{O}\Big(m^{-2}\Big)$$

with

$$b^2 = \frac{L}{2\pi}\frac{I_1^+ + I_1^-}{h} = \frac{L}{2\pi}\int_{\mathbb{T}_L} |\alpha(s)|^2\, \mathsf{e}^{-2\Im(\theta_1(s))}\, \frac{\eta_0(s)^{-1} + \eta_0(s)}{2\widehat{\tau}_0(s)}\mathrm{d}s > 0.$$

(iv) Revisiting the change of variables in tubular coordinates and the scaling, we get

$$\|\underline{R}_m\|_{\mathrm{L}^2(\Omega)} = h^{-2}\, \Big\| \mathsf{e}^{\mathsf{i}\, h^{-1}\, \Theta_h} \big(\mathcal{L}_h[a](\,\cdot\,, \Theta_h) - \Lambda_h\big)\, \big(\chi_h\, \Phi_h^-\big) \Big\|_{\mathrm{L}^2_-[h]}, \tag{4.18a}$$

$$\|\underline{R}_m\|_{\mathrm{L}^2(\mathbb{R}^2\setminus\overline{\Omega})} = h^{-2}\, \Big\| \mathsf{e}^{\mathsf{i}\, h^{-1}\, \Theta_h} \big(\mathcal{L}_h[a](\,\cdot\,, \Theta_h) - \Lambda_h\big)\, \big(\chi_h\, \Phi_h^+\big) \Big\|_{\mathrm{L}^2_+[h]} \tag{4.18b}$$

with $\mathcal{L}_h[a]$ defined in Equation (4.6). Lemma 4.8 with $N = 1$ and Lemma 4.3 give the estimation $\Im\big(\Theta_h\big) = \mathcal{O}(h)$, so there exists $c_\Theta > 0$ such that $|\mathsf{e}^{\mathsf{i}\, h^{-1}\, \Theta_h}| \leq c_\Theta$. Introducing the commutator $[\mathcal{L}_h[a](\,\cdot\,, \Theta_h), \chi_h]$ of the differential operator $\Phi \mapsto \mathcal{L}_h[a](\Phi, \Theta_h)$ with the scaled cut-off function χ_h, we deduce from Equation (4.18)

$$\|\underline{R}_m\|_{\mathrm{L}^2(\Omega)} \leq c_\Theta\, h^{-2}\, \big(\mathcal{N}_- + \mathcal{N}'_-\big) \quad \text{and} \quad \|\underline{R}_m\|_{\mathrm{L}^2(\mathbb{R}^2\setminus\overline{\Omega})} \leq c_\Theta\, h^{-2}\, \big(\mathcal{N}_+ + \mathcal{N}'_+\big), \tag{4.19}$$

where $\mathcal{N}_\pm = \|\chi_h \big(\mathcal{L}_h[a](\,\cdot\,, \Theta_h) - \Lambda_h\big)\, \Phi_h^\pm\|_{\mathrm{L}^2_\pm[h]}$ and $\mathcal{N}'_\pm = \|[\mathcal{L}_h[a](\,\cdot\,, \Theta_h), \chi_h]\, \Phi_h^\pm\|_{\mathrm{L}^2_\pm[h]}$. Let us start with $\mathcal{N}_\pm$. We write for $N \geq 1$,

$$\begin{aligned}\mathcal{L}_h[a](\Phi_h^\pm, \Theta_h) = \sum_{n=0}^{N-1} h^n \Big(\mathsf{L}_n^{\pm,3}(\Phi_h^\pm, \Theta_h, \Theta_h) + \mathsf{L}_n^{\pm,2}(\Phi_h^\pm, \Theta_h) + \mathsf{L}_n^{\pm,1}(\Phi_h^\pm)\Big) \\ + h^N \Big(\mathsf{R}_N^{\pm,3}(h; \Phi_h^\pm, \Theta_h, \Theta_h) + \mathsf{R}_N^{\pm,2}(h; \Phi_h^\pm, \Theta_h) + \mathsf{R}_N^{\pm,1}(h; \Phi_h^\pm)\Big)\end{aligned}$$

where $\mathsf{R}_N^{\pm,j}(h)$ are j-linear second-order differential operators such that all the coefficients in $\chi_h\, \mathsf{R}_N^{\pm,j}(h)$ are smooth bounded functions for $j \in \{1, 2, 3\}$. We use Lemma 4.8 with different N for each occurrence

of $\Phi_h^{\pm}$ and Θ_h, and we obtain

$$\begin{aligned}\mathcal{L}_h[a](\Phi_h^{\pm},\Theta_h) - \Lambda_h\Phi_h^{\pm} \\ = h^N\Bigg[\sum_{n=0}^{N-1}\sum_{p\in\mathbb{N}^3_{N-n}} \mathsf{L}_n^{\pm,3}\Big(R_{p_1}^{\pm}(h),R_{p_2}^{\Theta}(h),R_{p_3}^{\Theta}(h)\Big) + \mathsf{R}_N^{\pm,3}\big(h;R_0^{\pm}(h),R_0^{\Theta}(h),R_0^{\Theta}(h)\big) \\ + \sum_{n=0}^{N-1}\sum_{p\in\mathbb{N}^2_{N-n}} \mathsf{L}_n^{\pm,2}\Big(R_{p_1}^{\pm}(h),R_{p_2}^{\Theta}(h)\Big) + \mathsf{R}_N^{\pm,2}\big(h;R_0^{\pm}(h),R_0^{\Theta}(h)\big) \\ + \sum_{n=0}^{N-1}\Big(\mathsf{L}_n^{\pm,1} - \check{\lambda}_n\Big)R_{N-n}^{\pm}(h) + \mathsf{R}_N^{\pm,1}\big(h;R_0^{\pm}(h)\big) - R_N^{\Lambda}(h)R_0^{\pm}(h)\Bigg],\end{aligned} \tag{4.20}$$

where we used the relations in Equation (4.12), giving us that for all $Q\in\mathbb{N}$

$$\sum_{p\in\mathbb{N}^4_Q}\mathsf{L}_{p_1}^{3,\pm}\Big(\varphi_{p_2}^{\pm},\theta_{p_3},\theta_{p_4}\Big) + \sum_{p\in\mathbb{N}^3_Q}\mathsf{L}_{p_1}^{2,\pm}\Big(\varphi_{p_2}^{\pm},\theta_{p_3}\Big) + \sum_{p\in\mathbb{N}^2_Q}\Big(\mathsf{L}_{p_1}^{1,\pm} - \check{\lambda}_{p_1}\Big)\varphi_{p_2}^{\pm} = 0.$$

The coefficients in the operator $\chi_h\mathcal{L}_h[a](\cdot,\Theta_h)$ are smooth bounded functions in $\mathbb{T}_L\times\mathbb{R}_{\pm}$ (see Equations (4.8a), (4.8b) and (4.10). From Equation (20), we get $\mathcal{N}_{\pm}\le h^N\,\|F^{\pm}(h)\|_{\mathrm{L}_{\pm}[h]}$, where $F^{\pm}\in\mathscr{C}^{\infty}([0,\frac{L}{2\pi}]\times\mathbb{T}_L,\mathscr{S}(\mathbb{R}_{\pm}))$, so we have $\mathcal{N}_{\pm}\le C_N\,h^N$ for C_N a constant independent of h as $h\to 0$. Now, we consider the two commutator norms $\mathcal{N}'_{\pm}$. We observe that the coefficients of the operators $[\mathcal{L}_h[a](\cdot,\Theta_h),\chi_h]$ are zero in $\mathbb{T}_L\times(-\frac{\delta}{2h},0)$ and $\mathbb{T}_L\times(0,\frac{\delta}{2h})$. From this observation, we deduce that

$$\mathcal{N}'^{\,2}_{\pm} = \int_{\mathbb{T}_L}\int_{I_{\pm}(h)}|G^{\pm}(h;s,\rho)|^2\mathrm{d}\rho\mathrm{d}s,$$

where $G^{\pm}\in\mathscr{C}^{\infty}([0,\frac{L}{2\pi}]\times\mathbb{T}_L,\mathscr{S}(\mathbb{R}_{\pm}))$ and $I_{\pm}(h)$ are as in Lemma B.1 for $\rho=\frac{\delta}{2}$. We deduce that $\mathcal{N}'_{\pm}=\mathcal{O}(h^{\infty})$, and we get $\|\underline{R}_m\|_{\mathrm{L}^2(\Omega)}+\|\underline{R}_m\|_{\mathrm{L}^2(\mathbb{R}^2\setminus\overline{\Omega})}=\mathcal{O}\big(h^{N-2}\big)$ for all $N>1$.

(v) Let $(\theta_n)_{n\ge0}$ (resp. $(\vartheta_n)_{n\ge0}$) be a sequence of phases constructed for $\underline{u}_m$ (resp. $\underline{v}_m$) and α (resp. β) the function in Lemma 4.3. A similar computation as in *(iii)* gives that $\int_{\mathbb{R}^2}\underline{u}_m\,\overline{\underline{v}_m}\mathrm{d}x = z_0\,h+\mathcal{O}\big(h^2\big)$ where

$$\begin{aligned}z_0 &= \sum_{\pm}\int_{\mathbb{T}_L}\alpha(s)\overline{\beta(s)}\mathsf{e}^{\mathsf{i}\theta_1(s)-\mathsf{i}\overline{\vartheta_1(s)}}\int_{\mathbb{R}_{\pm}}\mathsf{e}^{\mp2\rho\,\widehat{\tau}_0(s)\eta_0(s)^{\mp1}}\mathrm{d}\rho\mathrm{d}s \\ &= \int_{\mathbb{T}_L}\alpha(s)\overline{\beta(s)}\,\mathsf{e}^{\mathsf{i}\theta_1(s)-\mathsf{i}\overline{\vartheta_1(s)}}\,\frac{\eta_0(s)^{-1}+\eta_0(s)}{2\widehat{\tau}_0(s)}\mathrm{d}s.\end{aligned}$$

From the expression of θ_1 and ϑ_1 in using Lemma B.2, we get $\mathsf{i}\theta_1(s)-\mathsf{i}\overline{\vartheta_1(s)} = -2f(s)-\int_0^s\frac{\alpha'(t)}{\alpha(t)}+\overline{\frac{\beta'(t)}{\beta(t)}}\mathrm{d}t$, where f is a real function independent of α and β. A derivative computation shows that the

functions

$$s \mapsto \alpha(s) \exp\left(-\int_0^s \frac{\alpha'(t)}{\alpha(t)} \mathrm{d}t\right) \equiv \alpha_0 \in \mathbb{C}^* \text{ and } s \mapsto \beta(s) \exp\left(-\int_0^s \frac{\beta'(t)}{\beta(t)} \mathrm{d}t\right) \equiv \beta_0 \in \mathbb{C}^*$$

are constant so $z_0 = \alpha_0 \overline{\beta_0} \int_{\mathbb{T}_L} \frac{\eta_0(s)^{-1} + \eta_0(s)}{2\widehat{\tau}_0(s)} \mathrm{e}^{-2f(s)} \mathrm{d}s \neq 0$. Denoting R (resp. S) the remainder in the construction of $\underline{u}_m$ (resp. $\underline{v}_m$), we have

$$\int_{\mathbb{R}^2} \underline{u}_m \, \underline{v}_m \mathrm{d}x = \int_{\mathbb{T}_L} F(h; s) \, \mathrm{e}^{\mathrm{i} \frac{4\pi m}{L} \theta_0(s)} \mathrm{d}s,$$

where

$$F(h; s) = \mathrm{e}^{\mathrm{i} R_1^{\Theta}(h;s) + \mathrm{i} S_1^{\Theta}(h;s)} \sum_{\pm} \int_{\mathbb{R}_\pm} \chi_u(h\rho) \chi_v(h\rho) R_0^{\pm}(h; s, \rho) S_0^{\pm}(h; s, \rho) h(1 + \rho\kappa(s)h) \mathrm{d}\rho.$$

Note that $F \in \mathscr{C}^\infty([0, \frac{L}{2\pi}] \times \mathbb{T}_L)$. Since $\theta_0' = \widehat{\tau}_0 > 0$, θ_0 is a smooth diffeomorphism from $\mathbb{T}_L$ to $\mathbb{T}_L$, we perform the change of variable $x = \theta_0(s)$

$$\int_{\mathbb{T}_L} F(h; s) \, \mathrm{e}^{\mathrm{i} \frac{4\pi m}{L} \theta_0(s)} \mathrm{d}s = \int_{\mathbb{T}_L} \left(\theta_0^{-1}\right)'(x) \, F\Big(h; \theta_0^{-1}(x)\Big) \, \mathrm{e}^{\mathrm{i} \frac{4\pi}{L} m x} \mathrm{d}x.$$

From the fact that the function $(h; x) \mapsto (\theta_0^{-1})'(x) \, F(h; \theta_0^{-1}(x)) \in \mathscr{C}^\infty([0, \frac{2\pi}{L}] \times \mathbb{T}_L)$ and the Riemann–Lebesgue lemma, we get

$$\int_{\mathbb{T}_L} \left(\theta_0^{-1}\right)'(x) \, F\Big(h; \theta_0^{-1}(x)\Big) \, \mathrm{e}^{\mathrm{i} \frac{4\pi}{L} m x} \mathrm{d}x = \mathcal{O}\big(m^{-\infty}\big).$$

□

We now add a correction to $\underline{u}_m$ in order to satisfy the transmission conditions. Consider $(\underline{\lambda}_m, \underline{u}_m)_{m \geq 1}$ in Equation (4.16), satisfying Lemma 4.9. We define

$$\breve{\underline{u}}_m(s, \xi) = \chi(\xi) \begin{cases} 0, & \text{if } \xi \leq 0, \\ [\underline{u}_m]_{\mathbb{T}_L \times \{0\}}(s) + \xi [a^{-1} \, \partial_\xi \underline{u}_m]_{\mathbb{T}_L \times \{0\}}(s), & \text{if } \xi > 0, \end{cases}$$

which gives $[\underline{u}_m - \breve{\underline{u}}_m]_\Gamma = 0$ and $[a^{-1} \, \partial_n \big(\underline{u}_m - \breve{\underline{u}}_m\big)]_\Gamma = 0$. Using the regularity and uniform compact support of $\underline{u}_m - \breve{\underline{u}}_m$, we obtain $\underline{u}_m - \breve{\underline{u}}_m \in \mathcal{D}(P)$. Using Lemma 4.9, we have $\|\breve{\underline{u}}_m\|_{\mathrm{L}^2(\mathbb{R}^2)} = \mathcal{O}(m^{-\infty})$ therefore $(P - \underline{\lambda}_m)(\underline{u}_m - \breve{\underline{u}}_m) = \mathcal{O}(m^{-\infty})$. We then replace $\underline{u}_m$ by

$$\underline{u}_m = \frac{\underline{u}_m - \breve{\underline{u}}_m}{\|\underline{u}_m - \breve{\underline{u}}_m\|_{\mathrm{L}^2(\mathbb{R}^2)}}, \tag{4.21}$$

which now makes $(\underline{\lambda}_m, \underline{u}_m)_{m\geq 1}$ a quasi-pair in the sense of Definition 2.2. To prove Theorem 2.3, we simply need to show that $(\underline{\lambda}_m)_{m\geq 1}$ are real and independent of the construction. To that aim we will check that $(\breve{\lambda}_n)_{n\geq 1}$ are real and unique (see Remark 4.7).

LEMMA 4.12. Let $(\underline{\lambda}_m, \underline{u}_m)_{m\geq 1}$ and $(\underline{\mu}_m, \underline{v}_m)_{m\geq 1}$ two quasi-pairs in the sense of Definition 2.2 corresponding to the same integer m and having the same leading order phase $\theta_0 \colon s \mapsto \int_0^s \widehat{\tau}_0(t)\mathrm{d}t$. Then we have the following estimate $\underline{\lambda}_m - \overline{\underline{\mu}_m} = \mathcal{O}\big(m^{-\infty}\big)$.

Proof. Let $\underline{R}_m$, $\underline{S}_m$ be the residuals $\underline{R}_m = P\underline{u}_m - \underline{\lambda}_m \underline{u}_m$ and $\underline{S}_m = P\underline{v}_m - \underline{\mu}_m \underline{v}_m$. By definition, the residuals satisfy $\|\underline{R}_m\|_{\mathrm{L}^2(\mathbb{R}^2)} = \mathcal{O}(m^{-\infty})$ and $\|\underline{S}_m\|_{\mathrm{L}^2(\mathbb{R}^2)} = \mathcal{O}(m^{-\infty})$. Using the symmetry of the operator P, we get

$$\Big(\underline{\lambda}_m - \overline{\underline{\mu}_m}\Big) \int_{\mathbb{R}^2} \underline{u}_m\, \overline{\underline{v}_m}\mathrm{d}x = \int_{\mathbb{R}^2} \underline{u}_m\, \overline{\underline{S}_m}\mathrm{d}x - \int_{\mathbb{R}^2} \underline{R}_m\, \overline{\underline{v}_m}\mathrm{d}x = \mathcal{O}\big(m^{-\infty}\big).$$

From Remark 4.10 one can show that there exists $z_0 \in \mathbb{C}^*$ such that $\int_{\mathbb{R}^2} \underline{u}_m\, \overline{\underline{v}_m}\mathrm{d}x = z_0 + \mathcal{O}(m^{-1})$. Then $\underline{\lambda}_m - \overline{\underline{\mu}_m} = \mathcal{O}(m^{-\infty})$ as $m \to +\infty$. □

COROLLARY 4.13. The quasi-resonances $(\underline{\lambda}_m)_{m\geq 1}$ are real and are independent of the construction.

Proof. By applying Lemma 4.12 to $(\underline{\lambda}_m, \underline{u}_m)_{m\geq 1}$ and $(\underline{\lambda}_m, \underline{u}_m)_{m\geq 1}$ we get $\Im\big(\underline{\lambda}_m\big) = \mathcal{O}(m^{-\infty})$ which implies that $\Im\Big(\breve{\lambda}_n\Big) = 0$ for all $n \in \mathbb{N}$. Then taking $(\underline{\lambda}_m, \underline{u}_m)_{m\geq 1}$ and $(\underline{\mu}_m, \underline{v}_m)_{m\geq 1}$ two quasi-pairs in the sense of Definition 2.2, from Remark 4.5, we can always assume that they have the same leading phase $\theta_0 \colon s \mapsto \int_0^s \widehat{\tau}_0(t)\mathrm{d}t$ (by taking $\overline{\underline{v}_m}$ instead of $\underline{v}_m$). Therefore, Lemma 4.12 and the fact that the quasi-resonances are real give us $\underline{\lambda}_m - \underline{\mu}_m = \mathcal{O}(m^{-\infty})$, which implies that $\breve{\lambda}_n = \breve{\mu}_n$. □

Results from Corollary 4.13, Lemma 4.9 and Equation (4.21) imply Theorem 2.3. In the next section we use Theorem 2.3 and the 'quasimodes to resonances' result to prove Theorem 2.4, Corollary 2.5 and Corollary 2.6. This establishes the connection between the quasi-pairs and the scattering resonances, plus their effect on the scattering instabilities. We end this section with a few remarks.

REMARK 4.14. With Corollary 4.13, given a quasi-pair $(\underline{\lambda}_m, \underline{u}_m)_{m\geq 1}$, we have a second quasi-orthogonal quasi-pair $(\underline{\lambda}_m, \overline{\underline{u}_m})_{m\geq 1}$ with the same quasi-resonance in the sense that, from *(v)* in Lemma 4.9, $\int_{\mathbb{R}^2} \underline{u}_m\, \overline{\overline{\underline{u}_m}}\mathrm{d}x = \mathcal{O}\big(m^{-\infty}\big)$. The quasi-resonances have an asymptotic multiplicity of 2, related to the chosen sign of the leading phase θ_0 (see Remark 4.5).

REMARK 4.15. We can generalize the hypothesis of Theorem 2.3 to complex-valued function $a_{\mathsf{c}} \in \mathscr{C}^\infty(\overline{\Omega}, \mathbb{C}^*)$ as long as $a_{\mathsf{c}}\big|_{\Gamma} \neq -1$ and $\rho \mapsto \varphi_0^{\pm}(s,\rho)$ in Lemma 4.3 are exponentially decreasing for $\rho \to \pm\infty$. In other words we need

$$\Re\Big(\widehat{\tau}_0(s)\, \eta_0(s)^{\pm 1}\Big) > 0 \qquad \text{where } \tau_0(s) = \Big(1 - \eta_0(s)^{-2}\Big)^{-\frac{1}{2}} \text{ and } \widehat{\tau}_0 = \frac{\tau_0}{\langle \tau_0 \rangle}$$

and considering the principal branch of the square root. However, if a_{c} is complex non-real, the operator P is non-self-adjoint and Lemma 4.12, Corollary 4.13, Remark 4.14 are not true anymore.

4.4 *First expansion terms of* $\underline{\lambda}_m$

We provide here a few terms of the asymptotic expansions of $\underline{\lambda}_m$ to identify their key features. The coefficients $\breve{\lambda}_n$ are computed using formulas in the proof of Lemma 4.6 via SymPy Meurer *et al.* (2017), and symbolic codes are available in the GitHub repository (Moitier & Carvalho, 2023).

4.4 *General cavity with varying coefficient.* We set the coefficients $\eta_0(s) = \eta(s,0)$ and $\eta_1(s) = \partial_\xi \eta(s,0)$; we obtain

$$\underline{\lambda}_m = \left(\frac{2\pi m}{L}\right)^2 \frac{\varsigma}{\langle \tau_0 \rangle^2}\left[1 - \left\langle \frac{\eta_0^2 - 1}{\eta_0}\kappa + \frac{\eta_1}{{\eta_0}^2(\eta_0^2 - 1)}\right\rangle\left(\frac{L}{2\pi m}\right) + \mathcal{O}\left(m^{-2}\right)\right]. \tag{4.22}$$

Looking at the first terms one can see that:

- The sign comes from the leading term and depends on $\varsigma = \operatorname{sign}(1 - \eta_0^2)$ (see Notation 4.1), namely on $a_{\mathsf{c}} < -1$ or $-1 < a_{\mathsf{c}} < 0$.
- The curvature κ appears only starting at the second term, it has a weak effect on the expansion.
- The terms blow up in the limit $\eta_0 \to 1$ (which corresponds to $a_{\mathsf{c}}|_\Gamma \to -1$). This is expected as for $a_{\mathsf{c}} \equiv -1$ since SPW correspond to zero eigenvalues.

One can compute higher order terms such as $\breve{\lambda}_2$, however it becomes rather cumbersome and lengthy to present here (expressions can be found in Moitier & Carvalho (2023)). We provide below a specific case where the expression $\breve{\lambda}_2$ is not too large.

4.4 *Circular cavity of radius R with radially varying coefficient* $\eta(r)$. Following previous results, we then set $\eta_0 = \eta(R)$, $\eta_1 = \partial_r \eta(R)$, $\eta_2 = \partial_r^2 \eta(R)$, and we obtain

$$\underline{\lambda}_m = \frac{m^2}{R^2}\left(1 - \eta_0^{-2}\right)\left[1 - \left(\frac{\eta_0^2 - 1}{\eta_0 R} + \frac{\eta_1}{\eta_0^2(\eta_0^2 - 1)}\right)\left(\frac{R}{m}\right) + \breve{\lambda}_2\left(\frac{R}{m}\right)^2 + \mathcal{O}\left(m^{-3}\right)\right], \tag{4.23}$$

where

$$\breve{\lambda}_2 = -\frac{(\eta_0^4 + 1)(\eta_0^4 - \eta_0^2 + 1)}{2\eta_0^4 R^2} + \frac{\eta_1(\eta_0^8 + 2\eta_0^6 - 3\eta_0^2 + 2)}{5\eta_0^5(\eta_0^4 - 1)R} - \frac{\eta_1^2(3\eta_0^4 + 4\eta_0^2 - 1)}{2\eta_0^6(\eta_0^4 - 1)} + \frac{\eta_2}{2\eta_0^3(\eta_0^2 - 1)}.$$

5. Black Box Scattering framework for unbounded transmission problems with sign-changing coefficient

5.1 *Proof of Theorem 2.4*

In this section, we prove Theorem 2.4. In the case (i): $a_{\mathsf{c}}(\gamma) < -1$ for all $\gamma \in \Gamma$, it is based on the 'quasimodes to quasi-resonances' result (in particular we follow the theorem of Tang and Zworski (Tang & Zworski, 1998)) from the black box scattering framework. In the case (ii): $-1 < a_{\mathsf{c}}(\gamma) < 0$ for all $\gamma \in \Gamma$, the proof is based on the spectral theorem for self-adjoint operators. We start by case (ii). The operator P is self-adjoint and $\mathbb{R}_-$ only contains discrete eigenvalues (see Lemma A.5). Then the

existence of quasi-pairs with $\underline{\lambda}_m < 0$, using (Helffer, 2013, Proposition 8.20), gives us

$$\operatorname{dist}\big(\underline{\lambda}_m, \operatorname{Spec}(P)\big) = \mathcal{O}\big(m^{-\infty}\big).$$

Therefore, there exists a sequence $\big(\ell_m\big)_{m\geq 1}$ such that $\ell_m \in \mathrm{i}\mathbb{R}_+$, ℓ_m^2 is a negative eigenvalue, and $\ell_m^2 = \underline{\lambda}_m + \mathcal{O}\big(m^{-\infty}\big)$. For the case (i), the proof is a direct consequence of the following elements:

- the operator $(P, \mathcal{D}(P))$ is a *black box Hamiltonian* in the sense of (Dyatlov & Zworski, 2019, Definition 4.1) (see Lemma 5.2);
- one can estimate the number of eigenvalues of the reference operator $P^\sharp$ (a truncated version of the operator P) defined in Definition 5.3 (see Lemma 5.4). This allows to establish that the set of resonances, which is discrete, is not too large (one can count them).

Remark 5.1. From Remark 4.14, we have two quasi-orthogonal quasi-pairs and, as in (Balac *et al.*, 2021, Theorem 7.D), we have two resonances close to the quasi-resonance. This will be illustrated in Section 6.

In what follows we prove Lemma 5.2 and Lemma 5.4. Let us denote $\mathbb{D} := B(0, R_0)$ the open disk of radius R_0 so that the cavity Ω is compactly embedded in $\mathbb{D}$. We denote $\mathbf{1}_{\mathbb{D}}$, $\mathbf{1}_{\mathbb{R}^2\setminus\overline{\mathbb{D}}}$ the restriction on $\mathbb{D}$, $\mathbb{R}^2 \setminus \overline{\mathbb{D}}$, respectively.

Lemma 5.2. The operator $(P, \mathcal{D}(P))$ on $\mathrm{L}^2(\mathbb{R}^2)$ is a black box Hamiltonian in the sense of (Dyatlov & Zworski, 2019, Definition 4.1), meaning that the following is satisfied:

(4.1.1) we have the orthogonal decomposition $\mathrm{L}^2(\mathbb{R}^2) = \mathrm{L}^2(\mathbb{D}) \oplus \mathrm{L}^2(\mathbb{R}^2 \setminus \overline{\mathbb{D}})$.

(4.1.4) the operator $(P, \mathcal{D}(P))$ is self-adjoint and $\mathbf{1}_{\mathbb{R}^2\setminus\overline{\mathbb{D}}}\mathcal{D}(P) \subset \mathrm{H}^2(\mathbb{R}^2 \setminus \overline{\mathbb{D}})$.

(4.1.5) outside $\mathbb{D}$ the operator is equal to the Laplacian.

(4.1.6) for all $v \in \mathrm{H}^2(\mathbb{R}^2)$ such that $v|_{B(0,R_0+\varepsilon)} \equiv 0$ for $\varepsilon > 0$ then $v \in \mathcal{D}(P)$.

(4.1.12) the operator $\mathbf{1}_{\mathbb{D}}\,(P + \mathrm{i})^{-1} : \mathrm{L}^2(\mathbb{R}^2) \to \mathrm{L}^2(\mathbb{D})$ is compact.

Proof. The condition (4.1.1) is satisfied by definition. The condition (4.1.4) is a consequence of Lemma A.5 and Lemma A.1. The condition (4.1.5) is satisfied by definition of $(P, \mathcal{D}(P))$: $\mathbf{1}_{\mathbb{R}^2\setminus\overline{\mathbb{D}}}(Pu) = -\Delta\Big(\mathbf{1}_{\mathbb{R}^2\setminus\overline{\mathbb{D}}}(u)\Big)$ for $u \in \mathcal{D}(P)$. The condition (4.1.6) is a consequence of Lemma A.1. For the condition (4.1.12), we define $A\colon \mathrm{L}^2(\mathbb{R}^2) \to \mathrm{L}^2(\mathbb{D})$, $u \mapsto \iota\mathbf{1}_{\mathbb{D}}\,(P + \mathrm{i})^{-1}$, with the embedding $\iota\colon \mathrm{H}^1(\mathbb{D}) \to \mathrm{L}^2(\mathbb{D})$. The operator A is compact because $-\mathrm{i}$ is in the resolvent set (Lemma A.5), the projection $\mathbf{1}_{\mathbb{D}}$ goes from $\mathcal{D}(P)$ to $\mathrm{H}^1(\mathbb{D})$ (Lemma A.1), and ι is compact (Brezis, 2011, Theorem 9.16). □

Now that the operator $(P, \mathcal{D}(P))$ is a black box Hamiltonian, the solutions of Equation (2.3) are well-defined: this means that we have $(\ell, u) \in \mathbb{C} \setminus \mathbb{R}_- \times \mathcal{D}(P)$ and Equation (2.3) fits in the black box scattering framework. Then we define the reference operator and estimate its eigenvalues. From Lemma 5.2 we deduce that Conditions (1), (2), (3) in Tang & Zworski (1998) are satisfied. Lemma 5.4 establishes that the last condition, Condition (4) in Tang & Zworski (1998), is satisfied.

DEFINITION 5.3. From the operator $(P, \mathcal{D}(P))$ on $\mathrm{L}^2(\mathbb{R}^2)$, we define the reference operator $(P^\sharp, \mathcal{D}(P^\sharp))$ on $\mathrm{L}^2\Big((\mathbb{R}/R_\sharp\mathbb{Z})^2\Big)$ with $R_\sharp > R_0$ by $P^\sharp \colon u \mapsto -\mathrm{div}\Big(a_\sharp^{-1}\,\nabla u\Big)$ and

$$\mathcal{D}(P^\sharp) = \Big\{u \in \mathrm{L}^2\Big((\mathbb{R}/R_\sharp\mathbb{Z})^2\Big) \mid P^\sharp u \in \mathrm{L}^2\Big((\mathbb{R}/R_\sharp\mathbb{Z})^2\Big)\Big\},$$

where $a_\sharp = a_\mathsf{c}\mathbf{1}_{\overline{\Omega}} + \mathbf{1}_{(\mathbb{R}/R_\sharp\mathbb{Z})^2\setminus\overline{\Omega}}$ is the 'restriction' of a to $(\mathbb{R}/R_\sharp\mathbb{Z})^2$.

LEMMA 5.4. The reference operator $(P^\sharp, \mathcal{D}(P^\sharp))$ is self-adjoint, has discrete spectrum and we have the following weak Weyl estimate

$$\mathrm{Card}\big(\mathrm{Spec}(P^\sharp) \cap [-\mu, \mu]\big) = \mathcal{O}(\mu) \qquad \text{for} \mu \geq 1.$$

Proof. The proof that the reference operator is self-adjoint is similar to the proof of Lemma A.5 (see also (Carvalho, 2015, Theorem 4.2)). The spectrum is discrete because $(\mathbb{R}/R_\sharp\mathbb{Z})^2$ is a compact set. The weak Weyl estimation comes from (Mandel *et al.*, 2022, Section 4), particularly from Corollary 8. The proofs are the same, one simply replaces $\mathrm{H}^1_0(\Omega)$ by the zero mean function in $\mathrm{H}^1\Big((\mathbb{R}/R_\sharp\mathbb{Z})^2\Big)$. □

Lemma 5.4 shows that Condition (4) in Tang & Zworski (1998) is satisfied with $n^\sharp = 2$. Now that the resonance set is well-defined and characterized by quasi-pairs, we can prove Corollary 2.5. We will use the following result:

LEMMA 5.5. For $k \in \mathbb{C} \setminus \mathbb{R}_-$, we denote $\mathfrak{Res}(k) \colon \mathrm{L}^2_{\mathrm{comp}}(\mathbb{R}^2) \to \mathcal{D}_{\mathrm{loc}}(P)$ the meromorphic continuation of the resolvent. For $k > 0$ and $\chi \in \mathscr{C}^\infty_{\mathrm{comp}}(\mathbb{R}^2)$, we define $\mathfrak{Res}_\chi(k) \colon \mathrm{L}^2(\mathbb{R}^2) \to \mathcal{D}(P)$ the cut-off resolvent by $\mathfrak{Res}_\chi(k) = \chi\mathfrak{Res}(k)\chi$, as in (Moiola & Spence, 2019, Section 3.2).

Proof. The meromorphic continuation of the resolvent is given by Theorem 4.4 in Dyatlov & Zworski (2019) and Lemma 5.2. □

5.2 *Proof of Corollary 2.5*

Let χ and $\widetilde{\chi}$ in $\mathscr{C}^\infty_{\mathrm{comp}}(\mathbb{R}^2)$ with $\chi,\ \widetilde{\chi} \equiv 1$ on an open neighborhood of $\overline{\Omega}$ such that $\mathrm{supp}(\widetilde{\chi}) \subset \{\chi = 1\}$. From the definition of the quasi-pair $\big(\underline{\lambda}_m,\ \underline{u}_m\big)_{m\geq 1}$, let $\underline{k}_m = \sqrt{\underline{\lambda}_m} > 0$ and $\underline{v}_m = \widetilde{\chi}\underline{u}_m/\|\widetilde{\chi}\underline{u}_m\|_{\mathrm{L}^2(\mathbb{R}^2)}$. The family $\big(\underline{k}_m^2,\ \underline{v}_m\big)_{m\geq 1}$ is still a quasi-pair, therefore we have $P\underline{v}_m - \underline{k}_m^2\underline{v}_m = \underline{R}_m$ with the estimation $\|\underline{R}_m\|_{\mathrm{L}^2(\mathbb{R}^2)} = \mathcal{O}\big(m^{-\infty}\big)$. Due to the fact that $\mathrm{supp}\big(\underline{v}_m\big)$, $\mathrm{supp}\big(\underline{R}_m\big) \subset \mathrm{supp}(\widetilde{\chi}) \subset \{\chi = 1\}$, we have $\underline{v}_m = \chi\underline{v}_m$ and $\underline{R}_m = \chi\underline{R}_m$. We obtain

$$\begin{aligned}\Big(P - \underline{k}_m^2\Big)\underline{v}_m = \underline{R}_m \quad &\Rightarrow \quad \underline{v}_m = \mathfrak{Res}\big(\underline{k}_m\big)\big(\underline{R}_m\big)\\ &\Rightarrow \quad \chi\underline{v}_m = \chi\mathfrak{Res}\big(\underline{k}_m\big)\big(\chi\underline{R}_m\big)\\ &\Rightarrow \quad \underline{v}_m = \mathfrak{Res}_\chi\big(\underline{k}_m\big)\big(\underline{R}_m\big).\end{aligned}$$

We deduce that for all $N \in \mathbb{N}$, there exists $C_N > 0$ such that

$$1 = \|\underline{v}_m\|_{\mathrm{L}^2(\mathbb{R}^2)} = \|\mathfrak{Res}_\chi\big(\underline{k}_m\big)\big(\underline{R}_m\big)\|_{\mathrm{L}^2(\mathbb{R}^2)} \leq \Big|\Big|\Big|\mathfrak{Res}_\chi\big(\underline{k}_m\big)\Big|\Big|\Big| C_N^{-1} m^{-N},$$

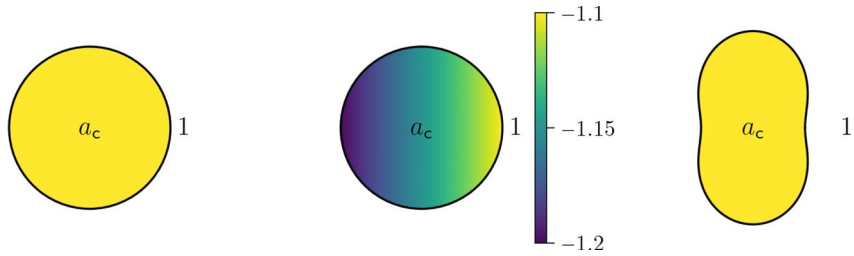

(A) Disk *(B) Disk, varying a_c* *(C) Peanut*

FIG. 8. Sketch representing the three considered configurations (A), (B) and (C), for the numerical illustration.

which gives the result.

REMARK 5.6. Results from Stefanov (2000) hold as well in this case: from families of resonances close to the positive real axis, we can create quasi-resonances.

5.3 *Proof of Corollary 2.6*

Now let $\underline{k}_m := \sqrt{\underline{\lambda}_m} > 0$ for $m \geq 1$. Results from Section 4 give us $-\mathrm{div}(a^{-1}\,\nabla \underline{u}_m) - \underline{k}_m^2 \underline{u}_m = \underline{R}_m$ with the remainder estimate $\|\underline{R}_m\|_{\mathrm{L}^2(\mathbb{R}^2)} = \mathcal{O}(m^{-\infty})$. Lemma A.4 with $g = 0$ and $f = \underline{R}_m$, gives us

$$\|\underline{u}_m\|_{\mathrm{L}^2(\mathbb{R}^2)} \leq C(\underline{k}_m)\ \|\underline{R}_m\|_{\mathrm{L}^2(\mathbb{R}^2)}.$$

Since $\|\underline{u}_m\|_{\mathrm{L}^2(\mathbb{R}^2)} = 1$ by definition and for all $N \geq 1$, there exists $\widetilde{c}_N > 0$ such that $\|\underline{R}_m\|_{\mathrm{L}^2(\mathbb{R}^2)} \leq \widetilde{c}_N m^{-N}$ then $\widetilde{c}_N^{-1}\, m^N \leq C(\underline{k}_m)$, for all $m \geq 1$.

6. Numerical illustration of metamaterial scattering resonances

Using Theorem 2.4 and Corollary 2.5 (proved in Section 5), we have shown that there exist scattering resonances located close to the positive real axis when $a_{\mathsf{c}}(\gamma) < -1$ for all $\gamma \in \Gamma$. Choosing $k = \Re(\ell)$ will lead to scattering instabilities for Equation (2.2). In what follows we provide several numerical examples showing the norm of the resolvent operator exploding close to scattering resonances. First we use the Finite Element Method (FEM) to compute the scattering resonances ℓ of the cavity close to the real axis (Step 1), then we compute the norm of the discretized cut-off resolvent operator for various k (Step 2). We also compare the scattering resonances with the first terms of the obtained asymptotic expansions (Step 3). We provide details about the steps below. We consider three cases:

(A) Circular cavity of radius 1 with constant $a_{\mathsf{c}} \equiv -1.1$ as represented in Fig. 8(a).

(B) Circular cavity of radius 1 with linearly varying permittivity $a_{\mathsf{c}}^{a_{\mathsf{m}},a_{\mathsf{M}}} : (x, y) \mapsto \frac{a_{\mathsf{m}}+a_{\mathsf{M}}}{2} + \frac{a_{\mathsf{M}}-a_{\mathsf{m}}}{2} x$, with $(a_{\mathsf{m}}, a_{\mathsf{M}}) = (-1.2, -1.1)$, as represented in Fig. 8(b).

(C) Peanut cavity with constant $a_{\mathsf{c}} \equiv -1.1$ as represented in Fig. 8(c). The peanut boundary is parameterized by $r(\theta) = 1 - \frac{3}{10}\cos(2\theta)$ with $\theta \in \mathbb{R}/2\pi\mathbb{Z}$.

Step 1: computing resonances. In order to solve Equation (2.3), we truncate the computational domain with a circular *perfectly matched layer* (PML) as done in Moitier (2019) (represented in green

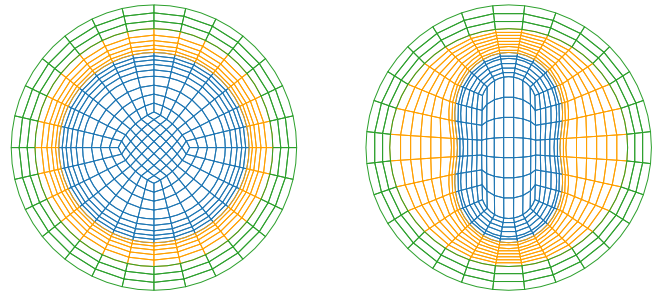

FIG. 9. Structured mesh for the circular cavity (left) and the peanut shape cavity (right). The cavity is represented in blue, the exterior domain in orange and the PML in green. The mesh is locally symmetric along the interface Γ. Meshes use quadrangular elements of degree 3, and we use finite elements of degree 8 in the computations (adding degrees of freedom in each element, not represented here).

Table 1 *Approximate value of the scattering resonances ℓ_{fem} in the three cases and for $m \in \{3, 6, 12\}$. The number of digits displayed is evaluated using an estimated numerical error, and we have put a '$*$' when the value is below the estimated error.*

ℓ_{fem}	$m = 3$	$m = 6$	$m = 12$
(A)	$1.1472 - \mathrm{i}10^{-2}$	$2.072 - \mathrm{i}10^{-3}$	$3.89308 - \mathrm{i}10^{*}$
	$1.1472 - \mathrm{i}10^{-2}$	$2.072 - \mathrm{i}10^{-3}$	$3.89308 - \mathrm{i}10^{*}$
(B)	$0.966 - \mathrm{i}10^{-1.6}$	$2.0681 - \mathrm{i}10^{-2}$	$4.21203 - \mathrm{i}10^{-5}$
	$0.966 - \mathrm{i}10^{-1.6}$	$2.0681 - \mathrm{i}10^{-2}$	$4.21231 - \mathrm{i}10^{-5}$
(C)	$0.46 - \mathrm{i}10^{-0.86}$	$1.5455 - \mathrm{i}10^{-1.91}$	$3.2954955 - \mathrm{i}10^{-3.32}$
	$0.93 - \mathrm{i}10^{-1.49}$	$1.6912 - \mathrm{i}10^{-2.65}$	$3.2990404 - \mathrm{i}10^{-4.44}$

in Fig. 9), and we consider T-conforming meshes (ad hoc locally symmetric meshes along the interface Γ) to guarantee FEM optimal convergence and avoid spurious eigenvalues (Bonnet-Ben Dhia *et al.*, 2013; Carvalho *et al.*, 2017). In practice, we build such meshes using GMSH Geuzaine & Remacle (2009) and consider quadrangular elements of degree 3 embedded in a tubular neighborhood as defined in Equation (4.1). We build a circular PML with radii $r_0 = 1.25$, $r_1 = r_0 + 0.25$ for the disk, and $r_0 = 1.25 \times 1.3$, $r_1 = r_0 + 0.25 \times 1.3$ for the peanut. After those transformations, the scattering resonances are approximated by the eigenvalues of the resulting FEM matrix, at least in a sector below the real axis (where the angle of the sector depends on the PML parameters).

The FEM computations are done using finite elements of degree 8 using XLiFE++ (2010), leading to 33 713 degrees of freedom for all three cases. Table 1 contains computed scattering resonances values ℓ_{fem} for various numbers of curvilinear oscillations $m \in \{3, 6, 12\}$, for the three cases. As mentioned in Remark 4.5, 4.14 and 5.1, for a given m, there are two resonances. We plot in Fig. 10 the two associated resonant modes for cases (B) and (C) associated with $m = 12$. One can observe that the size of angular oscillations changes when a_{c} varies (case (B)). Additionally, one observes that associated computed modes exhibit localized behaviours, as induced by SPW.

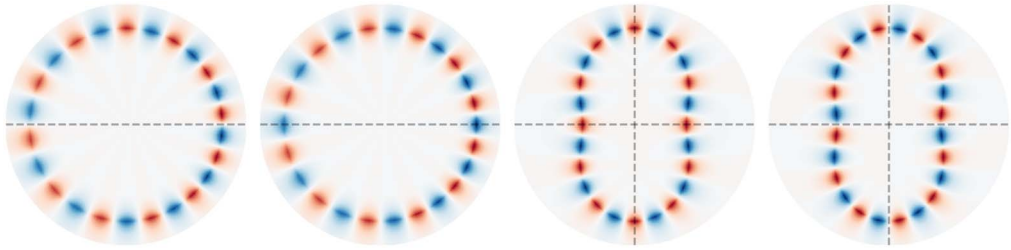

FIG. 10. Real part of the two resonant modes associated with $m = 12$ curvilinear oscillations, associated with the resonances in Table 1: for case (B) (left, middle left), for case (C) (middle right, right). The grey dashed lines represent the symmetry axes of the problem and hence the symmetries of the modes.

Step 2: norm of the discretized cut-off resolvent operator.

In Section 3 we computed the discrete norm of the reduced cut-off resolvent operator $\left|\left|\left|\mathbb{A}_k^{-1}\right|\right|\right|_2$, obtained using separation of variables. Here, we compute the discrete norm of a finite element version of the resolvent operator. We equivalently rewrite Equation (2.2) on a bounded domain using a Dirichlet-to-Neumann map (DtN), leading to Equation (A3) presented in Appendix A. We use FEM with T-conforming meshes such as the ones in Fig. 9 but without the PML to approximate Equation (A3), and we denote $\mathbb{M}_k$ the finite element matrix of the associated operator. Then we compute the associated discrete norm $\left|\left|\left|\mathbb{M}_k^{-1}\right|\right|\right|_2$ of the finite element cut-off resolvent operator using the spectral norm by a power method on $\left(\mathbb{M}_k^{\intercal}\right)^{-1}\mathbb{M}_k^{-1}$ on a uniform k-grid with geometric refinement around the real part of the scattering resonances.

The FEM computations are done using finite elements of degree 8 (leading to 28 337 degrees of freedom for all three cases), 65 Fourier modes for the DtN (Oberai *et al.*, 1998) and k-grids of 160 elements for case (A), 150 elements for cases (B) and (C) respectively.

Figure 11 presents results for case (A), where we can compare $\left|\left|\left|\mathbb{M}_k^{-1}\right|\right|\right|_2$ (dashed orange line) with $\left|\left|\left|\mathbb{A}_k^{-1}\right|\right|\right|_2$ (blue line) from the analytic computations in Section 3. Note that the numerical schemes used in both cases are not the same, hence we do not expect the results to identically match. However, the sharp peaks coincide exactly, they occur at $k = \Re\left(\ell_{\mathsf{fem}}\right)$ (ℓ_{fem} being the FEM scattering resonances computed in Step 1), and they exponentially grow as k increases (the y-axis is on a logarithmic scale). The grey vertical lines correspond to the real part of the scattering resonances ℓ_{fem}. For larger wavenumbers k, the FEM captures the scattering instabilities, but it fails to capture the peaks' intensity. This is due to the fact that the mesh is in this case not refined enough (despite high FEM order).

Figure 12 presents results for cases (B) and (C), where we do not have an analytic computation to compare with. As before, we observe that the norm of the cut-off resolvent operator peaks for $k = \Re\left(\ell_{\mathsf{fem}}\right)$ (indicated by the grey vertical lines in the figures), and the peaks grow exponentially with respect to k. As mentioned before, we have two resonant modes corresponding to the same number of curvilinear oscillations m, but they might have slightly different true resonances. For case (C), we clearly observe this phenomenon (double peaks). Note that for small m (*i.e.* small real part of the scattering resonances), the norm of the resolvent does not explode. This is due to scattering resonances having a more significant imaginary part.

Numerical results above illustrate the effect of scattering resonances induced by SPW, for various metamaterial cavities (in shape and in coefficient).

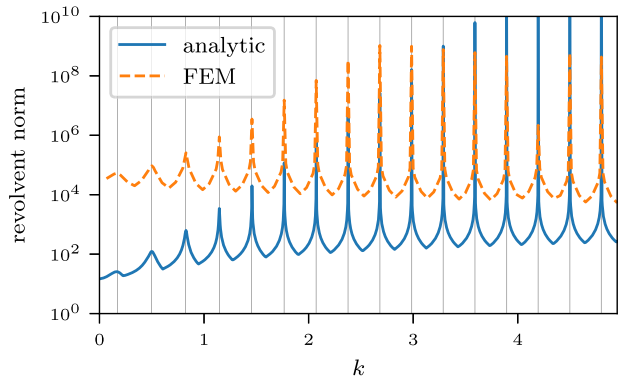

Case (A)

FIG. 11. Semi-log plot of the function $k \mapsto \|\mathbb{M}_k^{-1}\|_2$ for the disk cavity with $a_c = -1.1$. The blue line corresponds to the same analytic computation as in Section 3. The dotted orange lines correspond to FEM computations. The vertical grid lines are aligned on the real part of the scattering resonances.

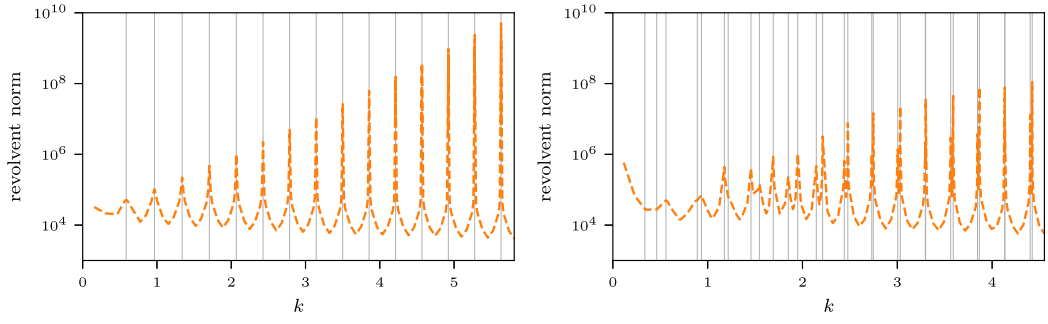

Case (B) *Case (C)*

FIG. 12. Semi-log plot of the function $k \mapsto \|\mathbb{M}_k^{-1}\|_2$ in logarithmic scale for the two cases *(B)* and *(C)*. The vertical grid lines are aligned on the real part of the scattering resonances.

Step 3: comparison with quasi-resonances. For validation purposes, we compare the scattering resonances ℓ_{fem} computed in Step 1 with $\sqrt{\underline{\lambda}_m}$, using $\underline{\lambda}_m$ defined in Equation (4.22). In particular, we will compare with the $\mathcal{O}(m^{-1})$, the $\mathcal{O}(m^{-2})$ expansion, respectively, which corresponds to choosing Equation (4.22) with one term, Equation (4.22) with two terms, respectively. We will denote them $\underline{\lambda}_{m,t}$, $t = 1, 2$. Recall that given m, resonances may be of multiplicity two: in that case we will add the superscript ^{s}, $s = 0, 1$, to distinguish between the two resonances. We now define the relative difference in scattering resonance with t terms at order m by

$$D_t^s(m) = \left| \frac{\sqrt{\underline{\lambda}_{m,t}^s} - \ell_{\mathsf{fem},m}^s}{\ell_{\mathsf{fem},m}^s} \right|, \quad s = 0, 1.$$

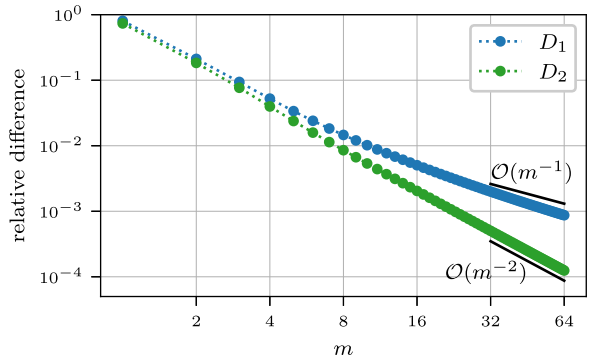

FIG. 13. Relative difference $D_t(m) := |\frac{\sqrt{\lambda_{m,t}}-\ell_m}{\ell_m}|$, $t = 1, 2$, between the scattering resonances $\ell_m \in \mathcal{R}_{\mathsf{pla}}[-1.1, 1]$ computed via the modal equation (Equation (3.5)), and the asymptotic expansion $\sqrt{\lambda_{m,t}}$ via Equation (4.22) for case (A).

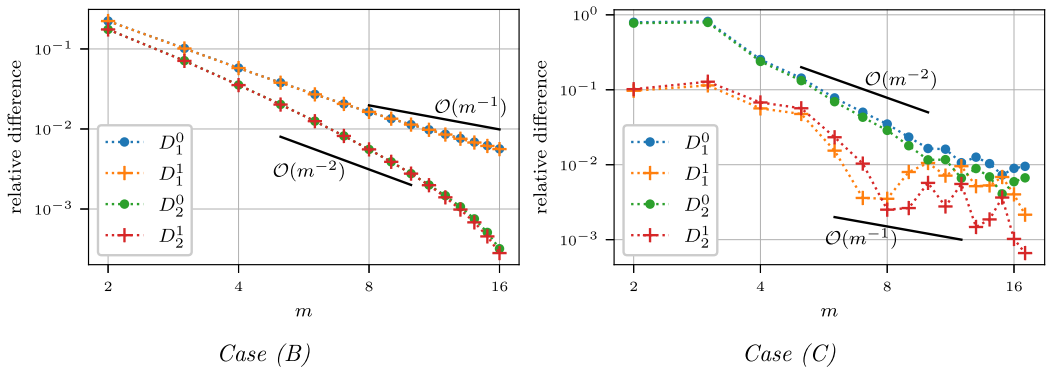

FIG. 14. Graphs of the relative difference $D_t^s(m)$, $s = 0, 1$, $t = 1, 2$, between the scattering resonances $\ell^s_{\mathsf{fem},m}$ computed via FEM (Step 1), and the asymptotic expansion $\sqrt{\lambda^s_{m,t}}$ via Equation (4.22), for cases (B) and (C).

Ideally, we expect that $\lim_{m\to+\infty} D_t^s(m) = \mathcal{O}(m^{-t})$, for $t = 1, 2$. Figures 13 and 14 represent $D_t^s(m)$ for cases (A), (B) and (C). In case (A), there is no multiplicity (we drop the superscript s), and we can use results from Section 3.1 to compare with the analytic scattering resonances $\ell_m \in \mathcal{R}_{\mathsf{pla}}[-1.1, 1]$. Figure 13 illustrates that ideal behaviour is reached. Figure 14 shows that, for cases (B) and (C), relative differences follows the anticipated slopes, which is promising (especially considering the range of m that may still be in pre-asymptotic regime). Further analysis of the asymptotic rates could be made (as done in (Moitier, 2019, Chpater 9)) to verify the asymptotic rates; this requires more computations. Overall, results from Figs 13 and 14 present reasonably small relative error between the scattering resonances and the quasi-resonances.

7. Conclusion

Similar to classical optical cavities, the scattering by negative metamaterial cavities can be significantly affected by localized waves at the boundary of the cavity. In this paper we have shown with the black box scattering framework that there exist metamaterial scattering resonances close to the positive real axis, causing the norm of resolvent operator to explode. Using asymptotic expansions, we have characterized those resonances to arbitrary order, and for various cavity properties (arbitrary smooth shape, varying negative permittivity, etc.). Numerical experiments illustrate that, for non-trapping metamaterial cavities, scattering resonances are associated with localized waves corresponding to SPW. This study has been carried out without reducing to the quasi-static case, and the considered spectral parameter is the wavenumber in contrast to Grieser (2014); Schnitzer (2019); Ammari *et al.* (2020a,b). Our asymptotic analysis revealed that, given some incident source associated with $k > 0$, surface plasmon waves can only be excited when $a_c < -1$ (in the case $-1 < a_c < 0$ the scattering resonances are purely imaginary). We have established that the 'quasimodes to quasi-resonances' result still applies for unbounded transmission problems with sign-changing coefficients: then the existence of quasi-pairs implies the existence of scattering resonances close to the positive real axis which also implies the explosion of the stability constant when $a_c < -1$. FEM computations confirm that the norm of the numerical resolvent operator exhibits high intensity narrow peaks associated with the scattering resonances close to the positive real axis.

Our approach provides the construction of SPW quasi-modes for general metamaterial cavities, to arbitrary order. The constructed quasi-modes seem to concur with resonant modes computed for non-trapping cavities. For trapping cavities, combinations of localized-trapped resonant modes could exist. The approach can be carried out for multi-layered cavities (typically a dielectric cavity surrounded by an annulus of metamaterial): one can build quasi-pairs for each interface (the localization process decouples phenomena). Then the 'quasimodes to quasi-resonances' argument should hold similar results. One could consider extracting those asymptotic plasmonic behaviours from the problem to relax FEM (no peaks), as done in the singular complement method Ciarlet & He (2003). One could also, using the same expansion methods, find asymptotic characterization in the context of dispersive material cavities (in particular the case where $a_c := \varepsilon_c$ is the permittivity and depends on the wavenumber k, such as Drude's or Lorentz' model). In that case, our analysis confirms that SPW waves can only be excited for frequencies lower than the surface plasmons' frequency (Maier, 2007); however, since the domain of the operator depends on the spectral parameter, the link between quasi-pairs and scattering resonances is not clear. Extensions to polygonal metamaterial cavities and dispersive metamaterials will be considered. In the quasi-static case, the spectral analysis for that case reveals hypersingular plasmonic behaviours and has been well investigated (Hazard & Paolantoni, 2020; Bonnet-Ben Dhia *et al.*, 2021). The proposed asymptotic expansions approach is valid for arbitrary optical parameter a_c (and complex-valued ones to some extent); one could also consider arbitrary double negative optical parameters b_c and work with the double-negative PDE $-\mathrm{div}(a^{-1}\nabla u) - b\,k^2\,u = 0$ (*e.g.* Bonnet-Ben Dhia *et al.* (2014); Fitzpatrick (2018); Ammari *et al.* (2019)). Then, to deduce from the quasi-pairs existence the presence of scattering resonances becomes difficult because the operator is no longer self-adjoint. All the derivations have been provided for two-dimensional problems; one could consider three-dimensional cavities. In particular, results from Appendix A and Section 5 hold in $\mathbb{R}^3$, for smooth interface Γ. The construction of quasi-pairs may be more cumbersome, but it can be adapted using a parameterized tubular region and the use of the mean curvature.

Acknowledgments

The authors would like to thank the reviewers for their helpful comments, C. Tsogka and A. D. Kim for their feedback and M. Dauge for the fruitful discussions.

Funding

This research was supported by the National Science Foundation Grant: DMS-2009366 and by the Deutsche Forschungsgemeinschaft (DFG, German Research Foundation)—Project-ID 258734477—SFB 1173.

References

Ammari, H., Millien, P., Ruiz, M. & Zhang, H. (2017) Mathematical analysis of plasmonic nanoparticles: the scalar case. *Arch. Rational Mech. Anal.*, **224**, 597–658. https://doi.org/10.1007/s00205-017-1084-5.

Ammari, H., Fitzpatrick, B., Lee, H., Yu, S. & Zhang, H. (2019) Double-negative acoustic metamaterials. *Quart. Appl. Math.*, **77**, 767–791. https://doi.org/10.1090/qam/1543.

Ammari, H., Chow, Y. T. & Liu, H. (2020a) Quantum ergodicity and localization of plasmon resonances. arXiv:2003.03696. http://arxiv.org/abs/2003.03696.

Ammari, H., Dabrowski, A., Fitzpatrick, B. & Millien, P. (2020b) Perturbation of the scattering resonances of an open cavity by small particles. Part I: the transverse magnetic polarization case. *Z. Angew. Math. Phys.*, **71** Paper No. 102, 21. https://doi.org/10.1007/s00033-020-01324-6.

Babič, V. M. & Buldyrev, V. S.. (1991) *Short-wavelength diffraction theory*, volume 4 of *Springer Series on Wave Phenomena*. Springer-Verlag, Berlin. *Asymptotic methods, Translated from the 1972 Russian original by E. F. Kuester*. https://doi.org/10.1007/978-3-642-83459-2.

Balac, S., Dauge, M. & Moitier, Z. (2021) Asymptotics for 2D whispering gallery modes in optical micro-disks with radially varying index. *IMA J. Appl. Math.*, **86**, 1212–1265. https://doi.org/10.1093/imamat/hxab033.

Bernardi, C., Dauge, M. & Maday, Y. (1999) *Spectral methods for axisymmetric domains*, volume 3 of *Series in Applied Mathematics (Paris)*. North-Holland, Amsterdam: Gauthier-Villars, Éditions Scientifiques et Médicales Elsevier, Paris Numerical algorithms and tests due to Mejdi Azaïez.

Bonnet-Ben Dhia, A.-S., Chesnel, L. & Ciarlet Jr., P. (2012) *T*-coercivity for scalar interface problems between dielectrics and metamaterials. *ESAIM Math. Model. Numer. Anal.*, **46**, 1363–1387. https://doi.org/10.1051/m2an/2012006.

Bonnet-Ben Dhia, A.-S., Chesnel, L. & Claeys, X. (2013) Radiation condition for a non-smooth interface between a dielectric and a metamaterial. *Math. Models Methods Appl. Sci.*, **23**, 1629–1662. https://doi.org/10.1142/S0218202513500188.

Bonnet-Ben Dhia, A.-S., Chesnel, L. & Ciarlet Jr., P. (2014) T-coercivity for the Maxwell problem with sign-changing coefficients. *Comm. Partial Differ. Equ.*, **39**, 1007–1031. https://doi.org/10.1080/03605302.2014.892128.

Bonnet-Ben Dhia, A.-S., Carvalho, C., Chesnel, L. & Ciarlet Jr., P. (2016) On the use of perfectly matched layers at corners for scattering problems with sign-changing coefficients. *J. Comput. Phys.*, **322**, 224–247. https://doi.org/10.1016/j.jcp.2016.06.037.

Bonnet-Ben Dhia, A.-S., Carvalho, C. & Ciarlet Jr., P. (2018) Mesh requirements for the finite element approximation of problems with sign-changing coefficients. *Numer. Math.*, **138**, 801–838. https://doi.org/10.1007/s00211-017-0923-5.

Bonnet-Ben Dhia, A.-S., Hazard, C. & Monteghetti, F. (2021) Complex-scaling method for the complex plasmonic resonances of planar subwavelength particles with corners. *J. Comput. Phys.*, **440** Paper No. 110433, 29. https://doi.org/10.1016/j.jcp.2021.110433.

Bonnetier, E., Dapogny, C., Triki, F. & Zhang, H. (2019) The plasmonic resonances of a bowtie antenna. *Analysis in Theory and Applications*, **35**, 85–116. https://doi.org/10.4208/ata.oa-0011.

Brezis, H. (2011) *Functional analysis, Sobolev spaces and partial differential equations*. Universitext. Springer, New York. https://doi.org/10.1007/978-0-387-70914-7.

Cacciapuoti, C., Pankrashkin, K. & Posilicano, A. (2019) Self-adjoint indefinite Laplacians. *J. Anal. Math.*, **139**, 155–177. https://doi.org/10.1007/s11854-019-0057-z.

Carvalho, C. (2015). *Étude mathématique et numérique de structures plasmoniques avec coins*. Theses, ENSTA ParisTech. https://pastel.archives-ouvertes.fr/tel-01240904.

Carvalho, C., Chesnel, L. & Ciarlet Jr., P. (2017) Eigenvalue problems with sign-changing coefficients. *C. R. Math. Acad. Sci. Paris*, **355**, 671–675. https://doi.org/10.1016/j.crma.2017.05.002.

Cho, J., Kim, I., Rim, S., Yim, G.-S. & Kim, C.-M. (2010) Outer resonances and effective potential analogy in two-dimensional dielectric cavities. *Phys. lett., A*, **374**, 1893–1899. https://doi.org/10.1016/j.physleta.2010.02.055.

Ciarlet Jr., P. & He, J. (2003) The singular complement method for 2d scalar problems. *C. R. Math. Acad. Sci. Paris*, **336**, 353–358. https://doi.org/10.1016/S1631-073X(03)00030-X.

Dyatlov S. and Zworski M. (2019). *Mathematical theory of scattering resonances, volume 200 of Graduate Studies in Mathematics* . American Mathematical Society, Providence, RI. https://doi.org/10.1090/gsm/200.

Fitzpatrick B. (2018) *Mathematical Analysis of Minnaert Resonances for Acoustic Metamaterials*. Theses, ETH Zurich. https://doi.org/10.3929/ethz-b-000287325.

Geuzaine, C. & Remacle, J.-F. (2009) Gmsh: a 3-D finite element mesh generator with built-in pre- and post-processing facilities. *Internat. J. Numer. Methods Engrg.*, **79**, 1309–1331. https://doi.org/10.1002/nme.2579.

Grieser, D. (2014) The plasmonic eigenvalue problem. *Rev. Math. Phys.*, **26**, 1450005, 26. https://doi.org/10.1142/S0129055X14500056.

Hazard, C. & Paolantoni, S. (2020) Spectral analysis of polygonal cavities containing a negative-index material. *Ann. H. Lebesgue*, **3**, 1161–1193. https://doi.org/10.5802/ahl.58.

Helffer, B. (2013) *Spectral theory and its applications, volume 139 of Cambridge Studies in Advanced Mathematics*. Cambridge: Cambridge University Press.

Helsing, J. & Karlsson, A. (2018) On a Helmholtz transmission problem in planar domains with corners. *J. Comput. Phys.*, **371**, 315–332. https://doi.org/10.1016/j.jcp.2018.05.044.

Hiptmair, R., Moiola, A. & Spence, E. A. (2022) Spurious quasi-resonances in boundary integral equations for the Helmholtz transmission problem. *SIAM J. Appl. Math.*, **82**, 1446–1469. https://doi.org/10.1137/21M1447052.

Hörmander L. (2003) *The analysis of linear partial differential operators. I*. Classics in Mathematics. Springer-Verlag, Berlin. *Distribution theory and Fourier analysis, Reprint of the second (1990) edition [Springer, Berlin]*. https://doi.org/10.1007/978-3-642-61497-2.

Kravanja P. and Van Barel M. (2000) *Computing the zeros of analytic functions, volume 1727 of Lecture Notes in Mathematics*. Springer-Verlag, Berlin. https://doi.org/10.1007/BFb0103927.

Maier S. A. (2007) *Plasmonics: Fundamentals and Applications*. Springer, New York, NY. https://doi.org/10.1007/0-387-37825-1.

Mandel, R., Moitier, Z. & Verfürth, B. (2022) Nonlinear Helmholtz equations with sign-changing diffusion coefficient. *C. R. Math. Acad. Sci. Paris*, **360**, 513–538. https://doi.org/10.5802/crmath.322.

Meurer, A., Smith, C. P., Paprocki, M., Čertík, O., Kirpichev, S. B., Rocklin, M., Kumar, A., Ivanov, S., Moore, J. K., Singh, S., Rathnayake, T., Vig, S., Granger, B. E., Muller, R. P., Bonazzi, F., Gupta, H., Vats, S., Johansson, F., Pedregosa, F., Curry, M. J., Terrel, A. R., Roučka, V., Saboo, A., Fernando, I., Kulal, S., Cimrman, R. & Scopatz, A. (2017) Sympy: symbolic computing in python. *PeerJ Computer Science*, **3**, e103. https://doi.org/10.7717/peerj-cs.103.

Moiola, A. & Spence, E. A. (2019) Acoustic transmission problems: wavenumber-explicit bounds and resonance-free regions. *Math. Models Methods Appl. Sci.*, **29**, 317–354. https://doi.org/10.1142/S0218202519500106.

Moitier, Z. (2019). Étude mathématique et numérique des résonances dans Une micro-cavité optique. *Theses, Université de Rennes*, **1**. http://www.theses.fr/en/2019REN1S053.

Moitier Z. and Carvalho C. (2023) *Asymptotic metacavity*. https://github.com/zmoitier/Asymptotic_metacavity. 10.5281/zenodo.4716361.

Moon, P. & Spencer, D. E. (1988) *Field theory handbook. Springer-Verlag, Berlin, second edition* Including coordinate systems, differential equations and their solutions.

Oberai, A. A., Malhotra, M. & Pinsky, P. M. (1998) Special Issue on Absorbing Boundary Conditions On the implementation of the dirichlet-to-neumann radiation condition for iterative solution of the helmholtz equation. *Appl. Numer. Math.*, **27**, 443–464. https://doi.org/10.1016/S0168-9274(98)00024-5.

Olver F. W. J., Lozier D. W., Boisvert R. F., and Clark C. W., editors (2010). *NIST handbook of mathematical functions. U.S. Department of Commerce, National Institute of Standards and Technology*, Washington, DC; Cambridge University Press, Cambridge. https://dlmf.nist.gov/.

Parini R. (2018) Cxroots: a python module to find all the roots of a complex analytic function within a given contour. https://github.com/rparini/cxroots.

Righini, G. C., Dumeige, Y., Féron, P., Ferrari, M., Conti, G. N., Ristic, D. & Soria, S. (2011) Whispering gallery mode microresonators: fundamentals and applications. *Riv. Nuovo Cimento*, **34**, 435–488. https://doi.org/10.1393/ncr/i2011-10067-2.

Sannomiya, T., Hafner, C. & Voros, J. (2008) In situ sensing of single binding events by localized surface plasmon resonance. *Nano Lett.*, **8**, 3450–3455. https://doi.org/10.1021/nl802317d.

Schnitzer, O. (2019) Geometric quantization of localized surface plasmons. *IMA J. Appl. Math.*, **84**, 813–832. https://doi.org/10.1093/imamat/hxz016.

Stefanov, P. (1999) Quasimodes and resonances: sharp lower bounds. *Duke Math. J.*, **99**, 75–92. https://doi.org/10.1215/S0012-7094-99-09903-9.

Stefanov, P. (2000) Resonances near the real axis imply existence of quasimodes. *C. R. Acad. Sci. Paris Sér. I Math.*, **330**, 105–108. https://doi.org/10.1016/S0764-4442(00)00105-1.

Stefanov, P. & Vodev, G. (1995) Distribution of resonances for the Neumann problem in linear elasticity outside a strictly convex body. *Duke Math. J.*, **78**, 677–714. https://doi.org/10.1215/S0012-7094-95-07825-9.

Stefanov, P. & Vodev, G. (1996) Neumann resonances in linear elasticity for an arbitrary body. *Comm. Math. Phys.*, **176**, 645–659. http://projecteuclid.org/euclid.cmp/1104286118.

Tang, S.-H. & Zworski, M. (1998) From quasimodes to resonances. *Math. Res. Lett.*, **5**, 261–272. https://doi.org/10.4310/MRL.1998.v5.n3.a1.

XLiF E++ (2010) *Librairie FEM-BEM C++, devellopée conjointement par les laboratoires IRMAR et POems*. https://uma.ensta-paristech.fr/soft/XLiFE++/.

Appendix A. Properties of the operator P

We recall the operator $P\colon u \mapsto -\mathrm{div}(a^{-1}\,\nabla u)$. Given $\omega \subseteq \mathbb{R}^2$, we define the bilinear form

$$b_\omega(u,v) = \int_\omega a^{-1}\nabla u \cdot \nabla v \,\mathrm{d}x, \quad u, v \in \mathrm{H}^1(\omega). \tag{A1}$$

Then $b := b_{\mathbb{R}^2}$ is the associated bilinear form of $(P, \mathcal{D}(P))$; one can write $b(u,v) = (Pu, v)_{\mathrm{L}^2(\mathbb{R}^2)}$ for $u \in \mathcal{D}(P)$, $v \in \mathrm{H}^1(\mathbb{R}^2)$, and is the associated bilinear form of Equation (2.2) for $\mathtt{P}\colon \mathrm{H}^1(\mathbb{R}^2) \to \mathrm{H}^{-1}(\mathbb{R}^2)$ ($b(u,v) = \langle \mathtt{P}u, v\rangle$ for $u, v \in \mathrm{H}^1(\mathbb{R}^2)$, where $\langle\cdot,\cdot\rangle$ is the duality bracket $\mathrm{H}^{-1}(\mathbb{R}^2) \times \mathrm{H}^1(\mathbb{R}^2)$).

Lemma A.1. The domain of P define by $\mathcal{D}(P) = \{u \in \mathrm{H}^1(\mathbb{R}^2) \,|\, \mathrm{div}\big(a^{-1}\nabla u\big) \in \mathrm{L}^2(\mathbb{R}^2)\}$ is equivalent to

$$\mathcal{D}(P) = \Big\{u \in \mathrm{H}^1\Big(\mathbb{R}^2\Big) \,|\, \Delta\, u|_\Omega \in \mathrm{L}^2(\Omega),\ \Delta\, u|_{\mathbb{R}^2\setminus\overline{\Omega}} \in \mathrm{L}^2\Big(\mathbb{R}^2 \setminus \overline{\Omega}\Big),\ [a^{-1}\partial_n u]_\Gamma = 0\Big\}.$$

Remark A.2. Without any assumption on the value of a_c on the interface Γ, we cannot expect H^2 regularity up to the interface, see e.g. (Cacciapuoti *et al.*, 2019, Theorem 1 and 2).

Proof. Let us denote

$$\mathcal{E} = \left\{ u \in \mathrm{H}^1\left(\mathbb{R}^2\right) \mid \Delta\, u|_{\Omega} \in \mathrm{L}^2(\Omega),\ \Delta\, u|_{\mathbb{R}^2\setminus\overline{\Omega}} \in \mathrm{L}^2\left(\mathbb{R}^2 \setminus \overline{\Omega}\right),\ [a^{-1}\partial_n u]_{\Gamma} = 0 \right\}.$$

For the inclusion $\mathcal{E} \subset \mathcal{D}(P)$, take $u \in \mathcal{E}$, using $[a^{-1}\partial_n u]_{\Gamma} = 0$ and Green's identity in a distributional sense, we have

$$\operatorname{div}\left(a^{-1}\,\nabla u\right) = \begin{cases} \operatorname{div}\left(a_{\mathtt{c}}^{-1}\nabla\, u|_{\Omega}\right) & \text{in } \Omega \\ \Delta\, u|_{\mathbb{R}^2\setminus\overline{\Omega}} & \text{in } \mathbb{R}^2 \setminus \overline{\Omega} \end{cases}$$

and with $\operatorname{div}(a_{\mathtt{c}}^{-1}\nabla\, u|_{\Omega}) = a_{\mathtt{c}}^{-1}\Delta\, u|_{\Omega} + \nabla(a_{\mathtt{c}}^{-1}) \cdot \nabla\, u|_{\Omega}$, it gives $\operatorname{div}\left(a^{-1}\,\nabla u\right) \in \mathrm{L}^2(\mathbb{R}^2)$. Therefore, we obtain $\mathcal{E} \subset \mathcal{D}(P)$. For the reciprocal inclusion, let us take $u \in \mathcal{D}(P)$ and $v \in \mathrm{H}^1(\mathbb{R}^2)$, using Green's identity and duality bracket, we get

$$\left\langle [a^{-1}\partial_n u]_{\Gamma},\ v|_{\Gamma} \right\rangle_{\mathrm{H}^{-1/2}(\Gamma),\,\mathrm{H}^{1/2}(\Gamma)} = b_{\mathbb{R}^2}(u,\,v) - (Pu, v)_{\mathrm{L}^2(\mathbb{R}^2)} = 0,$$

which gives $[a^{-1}\partial_n u]_{\Gamma} = 0$. With $\operatorname{div}\left(a^{-1}\nabla u\right) \in \mathrm{L}^2(\mathbb{R}^2)$, we get $\Delta\, u|_{\Omega} = a_{\mathtt{c}}[\operatorname{div}(a_{\mathtt{c}}^{-1}\nabla\, u|_{\Omega}) - \nabla(a_{\mathtt{c}}^{-1}) \cdot \nabla\, u|_{\Omega}] \in \mathrm{L}^2(\Omega)$ and $\Delta\, u|_{\mathbb{R}^2\setminus\overline{\Omega}} \in \mathrm{L}^2(\mathbb{R}^2 \setminus \overline{\Omega})$. □

Lemma A.3. If $a_{\mathtt{c}}(\gamma) \neq -1$, for all $\gamma \in \Gamma$, the bilinear form b_{ω} defined in Equation (A1) is weakly $\mathtt{T}$-coercive. More precisely, there exists an isomorphism $\mathtt{T} \in \mathcal{L}(\mathrm{H}^1(\omega))$, a compact operator $\mathtt{C} \in \mathcal{L}(\mathrm{L}^2(\omega))$, $\alpha > 0$ and $\beta \in \mathbb{R}$ such that b_{ω} satisfies a Gärding's inequality of the form:

$$b_{\omega}(u, \mathtt{T}u) \geq \alpha \|u\|^2_{\mathrm{H}^1(\omega)} - \beta \|\mathtt{C}u\|^2_{\mathrm{L}^2(\omega)}, \quad \forall u \in \mathrm{H}^1(\omega).$$

Proof. When $a_{\mathtt{c}} < 0$ is constant, one can use $\mathtt{T}$ provided in Bonnet-Ben Dhia *et al.* (2013) and the proof follows the one of (Bonnet-Ben Dhia *et al.* (2013), Lemma 2). When $a_{\mathtt{c}} \in \mathscr{C}^{\infty}(\Omega)$ non-constant, since $\partial\Omega$ is a smooth interface, it can always be seen as locally straight, then Theorems 3.10 and 4.3 in Bonnet-Ben Dhia *et al.* (2012) apply and provide the needed results. □

Lemma A.4. If $a_{\mathtt{c}}(\gamma) \neq -1$, for all $\gamma \in \Gamma$, the operator $\mathtt{P}$ is Fredholm of index 0 and Equation (2.2) is well-posed. Moreover, there exists a stability constant $C(k) > 0$ such that

$$\|u\|_{\mathrm{L}^2(\mathbb{D}(0,\rho))} \leq C(k)\left(\|f\|_{\mathrm{L}^2(\mathbb{R}^2)} + \|g\|_{\mathrm{L}^2(\Gamma)}\right), \tag{A2}$$

for any open disk of radius ρ such that $\overline{\Omega} \cup \operatorname{supp}(f) \subset \mathbb{D}(0, \rho)$.

Proof. Let $\mathbb{D}(0, \rho)$ be a disk a radius ρ such that Ω is compactly embedded in $\mathbb{D}(0, \rho)$, and $f \in \mathrm{L}^2(\mathbb{D}(0, \rho))$. Following Bonnet-Ben Dhia *et al.* (2016), we use a Dirichlet-to-Neumann map, denoted

$\mathcal{S}$, to rewrite Equation (2.2) in $\mathbb{D}(0,\rho)$: Find $u \in \mathrm{H}^1(\mathbb{D}(0,\rho))$ such that

$$\begin{cases} -\mathrm{div}\big(a^{-1}\,\nabla u\big) - k^2 u = f & \text{in } \mathbb{D}(0,\rho) \\ [u]_{\Gamma} = 0 \quad \text{and} \quad [a^{-1}\,\partial_n u]_{\Gamma} = g & \text{across } \Gamma \\ \partial_r u = \mathcal{S}u & \text{on } \partial\mathbb{D}(0,\rho) \end{cases} \tag{A3}$$

Lemma 1 in Bonnet-Ben Dhia *et al.* (2016) shows that problems Equation (A3)–(2.2) admits at most one solution. Following (Bonnet-Ben Dhia *et al.*, 2016, Section 2), using the properties of $\mathcal{S}$ and the fact that $\mathtt{K}\colon u \mapsto -k^2 u$ is compact, one simply needs to establish that the operator $\mathtt{P}\colon u \mapsto -\mathrm{div}\big(a^{-1}\,\nabla u\big)$ is Fredholm to conclude. From (Carvalho, 2015, Proposition 2.6), it is equivalent to show that $b|_{\mathbb{D}(0,\rho)}$ in Equation (A1) is weakly $\mathtt{T}$-coercive, which is established by Lemma A.3. Well-posedness of Equation (A3) in Hadamard's sense gives u that there exists $\widetilde{C}(k) > 0$ such that

$$\|u\|_{\mathrm{H}^1(\mathbb{D}(0,\rho))} \leq \widetilde{C}(k)\Big(\|g\|_{\mathrm{L}^2(\Gamma)} + \|f\|_{\mathrm{L}^2(\mathbb{D}(0,\rho))}\Big).$$

For Equation (2.2), using Poincaré's inequality this leads to

$$\|u\|_{\mathrm{L}^2(\mathbb{D}(0,\rho))} \leq C(k)\Big(\|g\|_{\mathrm{L}^2(\Gamma)} + \|f\|_{\mathrm{L}^2(\mathbb{R}^2)}\Big). \tag{A4}$$

□

Lemma A.5. If $a_{\mathtt{c}}(\gamma) \neq -1$, for all $\gamma \in \Gamma$, then $(P, \mathcal{D}(P))$ is self-adjoint, and its spectrum is such that $\mathrm{Spec}_{ess}(P) = \mathbb{R}_+$ and $\mathrm{Spec}_{dis}(P) \subset \mathbb{R}_-^*$.

Proof. The proof is given by applying Theorem 4.2, Propositions 4.5 and 4.6 in (Carvalho, 2015, Chapter 4). Consider $\lambda \in \mathbb{C} \setminus \mathbb{R}$ and the problem: Find $u \in \mathrm{H}^1(\mathbb{R}^2)$ such that $b(u,v) - \lambda(u,v)_{\mathrm{L}^2} = (f,v)_{\mathrm{L}^2}$, $\forall v \in \mathrm{H}^1(\mathbb{R}^2)$, with $f \in \mathrm{L}^2(\mathbb{R}^2)$. Using Lemma A.3, b is weakly $\mathtt{T}$-coercive and the above problem is well-posed (Lemma A.4). This shows that P is self-adjoint. Given $\lambda \in \mathrm{Spec}_{ess}(P)$, consider $(u_n)_n \in \mathcal{D}(P)$ such $\|u_n\|_{\mathrm{L}^2(\mathbb{R}^2)} = 1$, $u_n \rightharpoonup 0$ weakly in L^2 and such that $\|Pu_n - \lambda u_n\|_{\mathrm{L}^2} \to 0$. Using Lemma A.3, we have

$$\big(Pu_n, \mathtt{T}u_n\big)_{\mathrm{L}^2(\mathbb{R}^2)} \geq \alpha\|u_n\|^2_{\mathrm{H}^1(\mathbb{R}^2)} - \beta\|\mathtt{C}u_n\|^2_{L^2(\mathbb{R}^2)} \geq -\beta\|\mathtt{C}u_n\|^2_{\mathrm{L}^2(\mathbb{R}^2)},$$

and we note that

$$\big(Pu_n, \mathtt{T}u_n\big)_{\mathrm{L}^2(\mathbb{R}^2)} = \lambda(u_n, \mathtt{T}u_n)_{\mathrm{L}^2} = \lambda + \lambda(u_n, (\mathtt{T} - \mathrm{I})u_n)_{\mathrm{L}^2(\mathbb{R}^2)}.$$

Since $u_n \rightharpoonup 0$ weakly in L^2, one can show that $\|\mathtt{C}u_n\|^2_{\mathrm{L}^2(\mathbb{R}^2)} \to 0$, $(u_n, (\mathtt{T} - \mathrm{I})u_n)_{\mathrm{L}^2(\mathbb{R}^2)} \to 0$ strongly, which leads to $\lambda \geq 0$. On the other hand, for $\lambda \geq 0$, one can build a Weyl sequence $(u_n)_n \in \mathcal{D}(P)$ such $\|u_n\|_{\mathrm{L}^2(\mathbb{R}^2)} = 1$, $u_n \rightharpoonup 0$ weakly in L^2 and such that $\|Pu_n - \lambda u_n\|_{\mathrm{L}^2} \to 0$. Rellich lemma allows us to show that there are no eigenvalues in $\mathrm{Spec}_{ess}(P)$. Finally, P does not admit a lower bound (details can be found in (Carvalho, 2015, Section 4.2.2)): one can consider a sequence $(u_n)_n \in \mathcal{D}(P)$ with support strictly included in Ω such that the numerical range $(Pu_n, u_n)_{\mathrm{L}^2} \to -\infty$ (recall that $a_{\mathtt{c}} < 0$), which shows that $\mathrm{Spec}_{dis}(P) \subset \mathbb{R}_-^*$. □

Appendix B. Proofs and additional results for the asymptotic expansions

B.1 *Proof of Lemma 4.3*

Proof. We solve Equation (4.13) as ordinary differential equations with $s \in \mathbb{T}_L$ as a parameter. The conditions $\varphi_0^{\pm}(s,\cdot) \in \mathscr{S}(\mathbb{R}_{\pm})$ give the following restrictions $\theta_0'(s)^2 + \eta_0(s)^2\breve{\lambda}_0 \in \mathbb{C} \setminus \mathbb{R}_-$ and $\theta_0'(s)^2 - \breve{\lambda}_0 \in \mathbb{C} \setminus \mathbb{R}_-$. If one of the above restrictions is false, then there are no solutions $\varphi^{\pm}(s,\cdot)$ in $\mathscr{S}(\mathbb{R}_{\pm})$. Under those restrictions, there exists $\alpha(s), \beta(s) \in \mathbb{R}$ such that $\alpha(s)\beta(s) \neq 0$,

$$\varphi_0^-(s,\rho) = \alpha(s) e^{\rho\sqrt{\theta_0'(s)^2+\eta_0(s)^2\breve{\lambda}_0}}, \quad \text{and} \quad \varphi_0^+(s,\rho) = \beta(s) e^{-\rho\sqrt{\theta_0'(s)^2-\breve{\lambda}_0}},$$

where the square roots are chosen to be in $\mathbb{C}^{\frac{1}{2}}$. The first transmission condition $\varphi_0^-(s,0) = \varphi_0^+(s,0)$ implies that $\alpha(s) = \beta(s)$. Then the second transmission condition

$$-\eta_0(s)^{-2}\,\partial_\rho\varphi_0^-(s,0) = \partial_\rho\varphi_0^+(s,0)$$

give us

$$-\eta_0(s)^{-2}\sqrt{\theta_0'(s)^2 + \eta_0(s)^2\breve{\lambda}_0} = -\sqrt{\theta_0'(s)^2 - \breve{\lambda}_0},$$

leading to the eikonal equation

$$\theta_0'(s)^2 = \frac{\breve{\lambda}_0}{1-\eta_0(s)^{-2}} = \varsigma\breve{\lambda}_0\left|1-\eta_0(s)^{-2}\right|^{-1}.$$

While this equation does not have a unique solution, one simply selects one (see Remark 4.5). Here, we choose

$$\theta_0(s) = \sqrt{\varsigma\breve{\lambda}_0}\int_0^s \left|1-\eta_0(t)^{-2}\right|^{-\frac{1}{2}}\mathrm{d}t$$

and from the condition $\exp\left(\frac{\mathrm{i}}{h}\theta_0\right) \in \mathscr{C}^\infty(\mathbb{T}_L)$, we deduce that $\exp\left(\frac{\mathrm{i}}{h}\theta_0(L)\right) = \exp\left(\frac{\mathrm{i}}{h}\theta_0(0)\right)$ which implies that there exists $m \in \mathbb{N}$ such that

$$2\pi m = \frac{\theta_0(L)-\theta_0(0)}{h} = \frac{\sqrt{\varsigma\breve{\lambda}_0}}{h}\int_0^L \left|1-\eta_0(t)^{-2}\right|^{-\frac{1}{2}}\mathrm{d}t.$$

By choosing $h = \frac{L}{2\pi m}$ for $m \in \mathbb{N}^*$, we get $1 = \sqrt{\varsigma\breve{\lambda}_0}\langle|1-\eta_0^{-2}|^{-\frac{1}{2}}\rangle = \sqrt{\varsigma\breve{\lambda}_0}\langle\tau_0\rangle$ which gives $\breve{\lambda}_0 = \varsigma\langle\tau_0\rangle^{-2}$. Then with the relation $\tau_0^2 = \varsigma(1-\eta_0^{-2})^{-1}$ we obtain that

$$\sqrt{\theta_0'(s)^2 + \eta_0(s)^2\breve{\lambda}_0} = \widehat{\tau}_0(s)\,\eta_0(s) > 0 \quad \text{and} \quad \sqrt{\theta_0'(s)^2 - \breve{\lambda}_0} = \widehat{\tau}_0(s)\,\eta_0(s)^{-1} > 0,$$

which concludes the proof. □

B.2 *Proof of Lemma 4.6*

Proof. For $(s,\rho) \in \mathbb{T}_L \times \mathbb{R}_\pm$, we define $\mathsf{e}^\pm(s,\rho) = \exp\left(-|\rho|\,\widehat{\tau}_0(s)\,\eta_0(s)^{\mp 1}\right)$. We proceed by induction on n. For $n = 0$, Lemma 4.3 gives $(\varphi_0^\pm, \theta_0, \check{\lambda}_0)$ the solution of $(\mathcal{P}_0)$ defined in Equation (4.13). Let $n \geq 1$, from the definition of $S_{n-1}^\pm$ in Equation (15), there exists $Q_{n-1}^\pm \in \mathscr{C}^\infty(\mathbb{T}_L, \mathbb{P})$ such that $S_{n-1}^\pm = Q_{n-1}^\pm\,\mathsf{e}^\pm$. Using Lemma A.1 in Balac *et al.* (2021), we can solve the two ODEs in Equation (4.14) with the source terms $S_{n-1}^\pm$. We find that there exists $\widetilde{P}_n^\pm \in \mathscr{C}^\infty(\mathbb{T}_L, \mathbb{P})$ such that $\widetilde{\varphi}_n^\pm = \rho\widetilde{P}_n^\pm\,\mathsf{e}^\pm$, $\partial_\rho^2\widetilde{\varphi}_n^- - \widehat{\tau}_0^2\,\eta_0^2\,\widetilde{\varphi}_n^- = \eta_0^2\,S_{n-1}^-$, and $\partial_\rho^2\widetilde{\varphi}_n^+ - \widehat{\tau}_0^2\,\eta_0^{-2}\,\widetilde{\varphi}_n^+ = -S_{n-1}^+$. Then, solving the two ODEs in Equation (4.14) with the source terms $(2\widehat{\tau}_0\theta_0' + \eta_0^2\check{\lambda}_n)\varphi_0^-$ and $(2\widehat{\tau}_0\theta_0' - \check{\lambda}_n)\varphi_0^-$, for $(s,\rho) \in \mathbb{T}_L \times \mathbb{R}_\pm$, we obtain

$$\varphi_n^-(s,\rho) = \alpha(s)\rho\left(\frac{\eta_0(s)\,\check{\lambda}_n}{2\widehat{\tau}_0(s)} + \frac{\theta_n'(s)}{\eta_0(s)} + \frac{\widetilde{P}_n^-(s,\rho)}{\alpha(s)}\right)\mathsf{e}^-(s,\rho), \tag{B1a}$$

$$\varphi_n^+(s,\rho) = \alpha(s)\rho\left(\frac{\eta_0(s)\,\check{\lambda}_n}{2\widehat{\tau}_0(s)} - \eta_0(s)\,\theta_n'(s) + \frac{\widetilde{P}_n^+(s,\rho)}{\alpha(s)}\right)\mathsf{e}^+(s,\rho). \tag{B1b}$$

The first transmission condition $\varphi_n^-(\cdot,0) = \varphi_n^+(\cdot,0)$ is satisfied because $\varphi_n^\pm(\cdot,0) = 0$. Using the second transmission condition $-\eta_0^{-2}\,\partial_\rho\varphi_n^-(\cdot,0) = \partial_\rho\varphi_n^+(\cdot,0)$ and the expressions in Equation (B1), we get

$$-\eta_0^{-2}\left(\frac{\eta_0(s)\,\check{\lambda}_n}{2\widehat{\tau}_0(s)} + \frac{\theta_n'(s)}{\eta_0(s)} + \frac{\widetilde{P}_n^-(s,0)}{\alpha(s)}\right) = \frac{\eta_0(s)\,\check{\lambda}_n}{2\widehat{\tau}_0(s)} - \eta_0(s)\,\theta_n'(s) + \frac{\widetilde{P}_n^+(s,0)}{\alpha(s)}.$$

Solving for θ_n' and integrating yields

$$\theta_n(s) = \int_0^s \frac{\check{\lambda}_n}{2\widehat{\tau}_0(t)(1-\eta_0(t)^{-2})} + \frac{\eta_0(t)\widetilde{P}_n^-(t,0) + \eta_0(t)^3\widetilde{P}_n^+(t,0)}{\alpha(t)\,(\eta_0(t)^4 - 1)}\mathrm{d}t.$$

Now, the condition $\exp(\mathrm{i}\,h^{n-1}\,\theta_n) \in \mathscr{C}^\infty(\mathbb{T}_L)$ imposes $\theta_n(L) = \theta_n(0)$, solving for $\check{\lambda}_n$ and using the relation $\tau_0(t)^2\,(1-\eta_0^{-2}) = \varsigma$ yields

$$\check{\lambda}_n = -\frac{2\,\varsigma}{\langle\tau_0\rangle^2}\left\langle\frac{\eta_0\widetilde{P}_n^-(\cdot,0) + \eta_0^3\widetilde{P}_n^+(\cdot,0)}{\alpha\,(\eta_0^4 - 1)}\right\rangle.$$

Setting $P_n^\pm(s,\rho) = \alpha(s)\rho\left(\frac{\eta_0(s)\,\check{\lambda}_n}{2\widehat{\tau}_0(s)} \mp \eta_0(s)^{\pm 1}\theta_n'(s) + \frac{\widetilde{P}_n^\pm(s,\rho)}{\alpha(s)}\right)$ finishes the proof. □

B.3 *Additional results for Schwartz functions*

LEMMA B.1. Consider $F\colon (h;s,\rho)\mapsto F(h;s,\rho)$ in $\mathscr{C}^\infty([0,\frac{L}{2\pi}]\times\mathbb{T}_L,\mathscr{S}(\mathbb{R}_\pm))$, $\rho>0$, and the intervals $I_-(h)=(-\infty,-\frac{\rho}{h})$ and $I_+(h)=(\frac{\rho}{h},+\infty)$. Then

$$\int_{\mathbb{T}_L}\int_{I_\pm(h)}|F(h;s,\rho)|^2\mathrm{d}\rho\mathrm{d}s=\mathcal{O}(h^\infty)\quad\text{as } h\to 0.$$

Proof. Notice that, for any integer $N\geq 1$, there exists a constant $C_N>0$ such that $|\rho^N F(h;s,\rho)|\leq C_N$ for all $(h;s,\rho)\in[0,\frac{L}{2\pi}]\times\mathbb{T}_L\times\mathbb{R}_\pm$. Hence,

$$\int_{\mathbb{T}_L}\int_{I_\pm(h)}|F(h;s,\rho)|^2\mathrm{d}\rho\mathrm{d}s\leq\frac{C_N\,L}{(2N-1)\,\rho^{2N-1}}\,h^{2N-1},$$

which finishes the proof. □

B.4 *Additional results used in Section 4*

LEMMA B.2. For $s\in\mathbb{T}_L$,

$$\theta_1(s)=\int_0^s\frac{\check{\lambda}_1}{\check{\lambda}_0}\widehat{\tau}_0(t)+\frac{(\eta_0(t)^2-1)\,\kappa(t)}{2\,\eta_0(t)}+\frac{\eta_1(t)}{2\,\eta_0(s)^2\,(\eta_0(t)^2-1)}$$
$$+\mathrm{i}\,\frac{(\eta_0(t)^4+3)\,\eta_0'(t)}{2\,\eta_0(t)\,(\eta_0(t)^4-1)}+\mathrm{i}\,\frac{\alpha'(t)}{\alpha(t)}\mathrm{d}t.$$

Proof. This follows from the computation performed in Appendix B.2 where we solve Equation (4.14) for $n=1$ with

$$\eta_0^2 S_0^-=2\rho\frac{\eta_1}{\eta_0}\partial_\rho^2\varphi_0^--\left(\kappa-\frac{2\eta_1}{\eta_0}\right)\partial_\rho\varphi_0^--2\mathrm{i}\theta_0'\partial_s\varphi_0^-$$
$$-\left(2\rho{\theta_0'}^2\left(\kappa+\frac{\eta_1}{\eta_0}\right)+\mathrm{i}\theta_0'-2\mathrm{i}\theta_0'\frac{\eta_0'}{\eta_0}\right)\varphi_0^-,$$
$$-S_0^+=-\kappa\,\partial_\rho\varphi_0^+-2\mathrm{i}\theta_0'\partial_s\varphi_0^+-\left(2\rho{\theta_0'}^2\kappa+\mathrm{i}\theta_0'\right)\varphi_0^+.$$

□